Contract No. : K 2313-06-0015

SOCAAR Report No. : CR-WB-2007-02

Data Analysis and Source Apportionment of $PM_{2.5}$ in Golden, British Columbia using Positive Matrix Factorization (PMF)

A final report for a research contract between

Environment Canada

and

The University of Toronto

Authors : Professor Greg J. Evans

Dr. Cheol-Heon Jeong

Southern Ontario Centre for Atmospheric Aerosol Research

University of Toronto

Submitted: April 30, 2007

200 College Street

Toronto, ON, M5S-3E5, Canada

Tel: (416) 978-1821; Fax: (416) 978-8605

e-mail: evansg@chem-eng.toronto.edu

TABLE OF CONTENTS

LIST OF FIGURES

LIST OF TABLES

EXECUTIVE SUMMARY

This report outlines the methodology and findings from a three-month research contract to interpret particulate matter speciation data from Golden, British Columbia (B.C.). The focus of this project was the application of receptor modeling techniques to identify the origins of the particulate matter (PM).

Positive Matrix Factorization (PMF), a useful factor analysis method, was applied to 24-hr PM speciation data collected between November 2004 and August 2006 to identify possible sources of PM and determine the contribution of each identified source to ambient PM concentrations in Golden. Uncertainty estimates for the data including missing and below detection limit data were constructed to reflect the quality and reliability of each result. In addition to the point-by-point estimates of uncertainty, a signal-to-noise ratio for each element was calculated so that down-weighting of noisy variables could be taken into account in the PMF model application. PMF apportioned the $PM_{2.5}$ mass into seven factors identified as road salt, secondary sulphate, wood burning, wood processing, crustal material, traffic, and winter heating. The most important sources affecting ambient air quality in Golden were wood burning and winter heating factors.

In order to obtain the quantitative contributions for the sources, their relative contributions were normalized through multiple linear regression against the aerosol mass concentration. In addition, seasonal trends of the PMF-resolved sources were characterized. The identity of the sources was further elucidated by exploring their relationship with other measured parameters; a correlation study was conducted to evaluate relationships between the sources, volatile organic compounds, gaseous pollutants, and meteorological variables.

1. INTRODUCTION

Numerous epidemiological studies have shown that increased concentration of airborne particulate matter (PM), especially in particles smaller than 2.5 μm in aerodynamic diameter ($PM_{2.5}$) and particles smaller than 10 μm in aerodynamic diameter (PM_{10}), are associated with increased mortality, increased hospitalization for respiratory and cardiovascular diseases, increased respiratory symptoms, and reduced lung function (e.g., Dockery et al. 1993; Burnett et al. 2000). In addition to adverse health effects, visibility reduction by light-extinction as well as the radiation balance of the Earth are associated with the chemical composition of particles in certain size ranges (Cadle and Mulawa 1990). Characterization of PM chemical composition variation is important not only to understand adverse health effects of chemical species, but also to identify aerosol sources and their contributions. Fine particles are usually formed from combustion sources and photochemical reactions followed by gas to particle conversion. These particles mainly consist of carbonaceous compounds, sulphate, nitrate, and other trace metals. In contrast, coarse particles are usually formed from mechanical processes including dust resuspension, and typically contain high concentrations of crustal elements.

Observations of the chemical compositions of PM in the atmosphere is essential for understanding aerosol physical and chemical processes and identifying possible sources of ambient particles. The sources of PM can be derived by statistical techniques from source oriented air quality models, chemical mass balance (CMB) methods and receptor modeling. In the CMB model, the contributions of the sources are estimated based on prior information such as the number of possible sources and the chemical composition of each source. Airborne particle sources, however, are unknown for most locations and the chemical composition data of particles emitted from the sources are usually not available. Compared to the CMB, Positive Matrix Factorization (PMF, Paatero 1997), a type of bilinear multivariate receptor modeling, can be applied to identify PM sources and provide the contribution of each source in the absence of prior information on sources. Most locations receive $PM_{2.5}$ from local and regional sources. Regional and local source contributions to $PM_{2.5}$ have been apportioned by using PMF in many ambient aerosol studies at urban sites (e.g., Chueinta et al. 2000; Polissar et al. 2001; Lee et al.

2003). Receptor modeling provides a method to distinguish the relative contributions of different sources based upon measurements collected at a site. Specifically, temporal variations in the speciation of the particulate matter can be used to identify associations between components, thereby allowing the potential source composition, the source profile, to be approximated. Applying a mass balance in relation to these source profiles allows the mass contribution of each source to be estimated. The presence of marker elements, along with the examination of seasonal and diurnal trends in resolved factors, can allow these sources to be named. Coupling with other pollutant data, such as pollutant gases, the source identification can be further refined. Use of meteorological data such as wind direction and back-trajectories can provide more insight into the geographic location of the sources. Recently, the EPA has developed a graphical user interface version of PMF (EPA PMF) and freely distributed it (Eberly 2005). Based on the PMF model, EPA PMF uses an algorithm known as Multilinear Engine (ME2, Pattero 1999) to characterize and apportion PM sources.

In Golden, a typical valley site of British Columbia, Canada, PM_{10} concentrations historically exceeded provincial 24-hour averages over the winter months. Recently, the growing concerns have been given to the PM sources and their contributions, especially during high PM episodes in winter. A Canada-wide Standard (CWS) for $PM_{2.5}$ has been developed. It is based upon a 98^{th} percentile value of 30 $\mu g\ m^{-3}$ for a 24-hour average, determined over 3 year of measurements. Research into the sources and causes of high $PM_{2.5}$ level is needed to develop strategies for improving air quality and to ensure that the CWS is met by the required time, 2010. A recent study conducted by Environment Canada found that in winter a leading contributor to PM with aerodynamic diameter < 1 μm (PM_1) was wood burning related activities in the Golden area (Submitted for Publication by Dr. Jeffrey Brook). Determination of wood burning-related sources and temporal contributions to the ambient concentration of $PM_{2.5}$ is the most important step in the development of anthropogenic emission control strategies in the typical valley area. To better understand the sources of $PM_{2.5}$, particularly residential wood combustion, comprehensive aerosol sampling was conducted for twenty-two months in Golden.

This report describes the application of source-receptor modeling to the results of this sampling.

To quantitatively estimate the mass contributions of identified sources, the relative contributions of resolved sources were normalized through multiple linear regression against the total aerosol mass. In order to identify the most probable direction of local point sources, Conditional Probability Function (CPF) was perform using wind direction data and resolved source contributions in this work. Furthermore, a correlation study was conducted to evaluate relationships between the resolved source contributions, levoglucosan (a typical molecular organic marker for biomass burning), gaseous pollutants including Volatile Organic Compounds (VOCs), meteorological variables, and vehicle numbers. This analysis serves to improve the interpretation of identified sources. Lastly, a comparison between PMF and EPA PMF in terms of source profiles and contributions at the Golden site is discussed.

2. EXPERIMENTAL AND METHODOLOGY

2.1 Site Description

All samples in this study were collected at the downtown site in Golden, British Columbia (B.C.), one of National Air Pollution Surveillance (NAPS) sites operated by the British Columbia Ministry of Environment. Golden is in eastern B.C., about 100 km west of Banff, Alberta, located at the junction of Highway 95 and the Trans-Canada Highway 1, bound by Glacier National Park to the west and Yoho National Park to the east, where wind and air circulation is typically suppressed (Figure 1). Due to the unique topographic influence, temperature inversion frequently occurred in the winter and the predominant wind directions are from northwest and southeast as shown in Figure 2. On average, wind speed in summer (2.3 ± 2.0 m/sec, average ± standard deviation) was higher than in winter (1.3 ± 0.9 m/sec) with an annual average of 1.7 ± 1.4 m/sec. The ratio of minium to maximum values on the diurnal variations of wind speeds in summer (June to August) and in winter (December to January) were 2.53 and 1.50, respectively. The higher ratio indicates significant diurnal changes in the atmospheric boundary layer in the summer months, as expected.

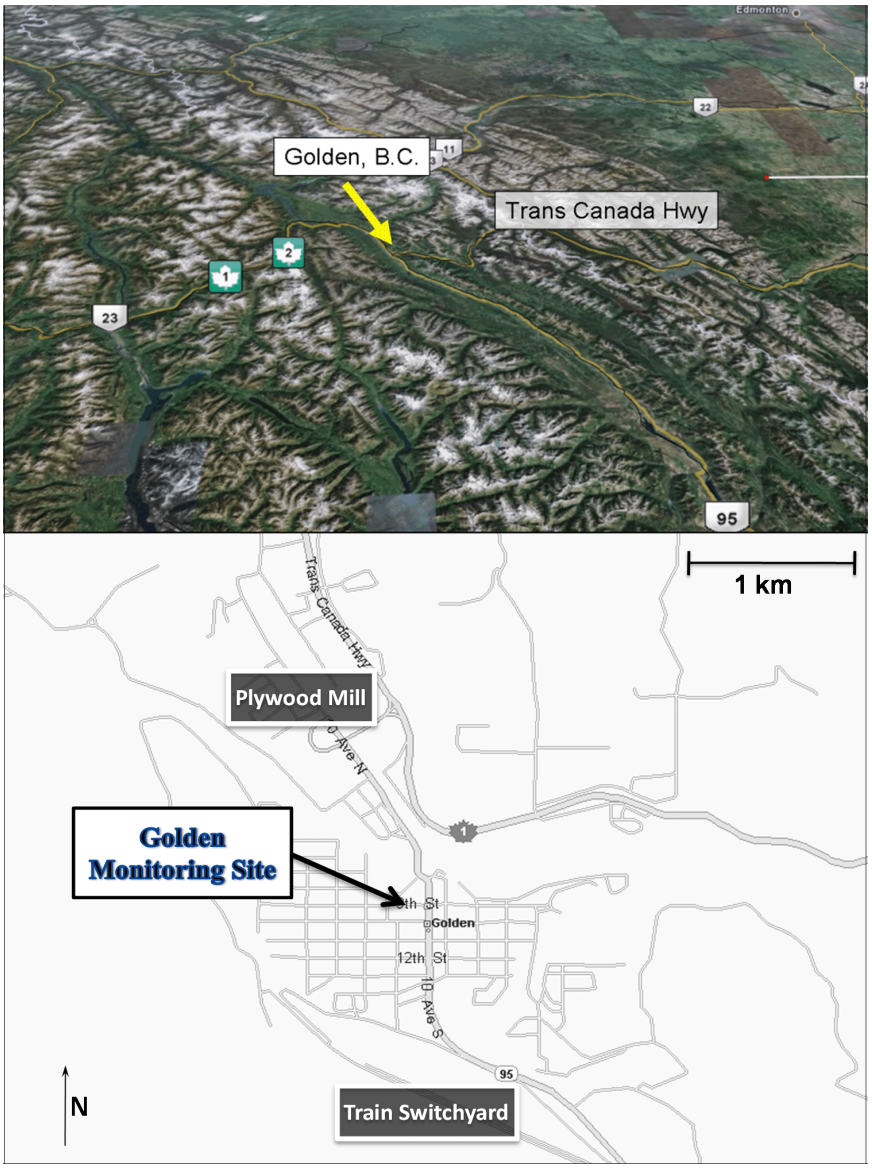

Figure 1. Map of the monitoring site and the local sources of emissions in Golden. B.C. Canada

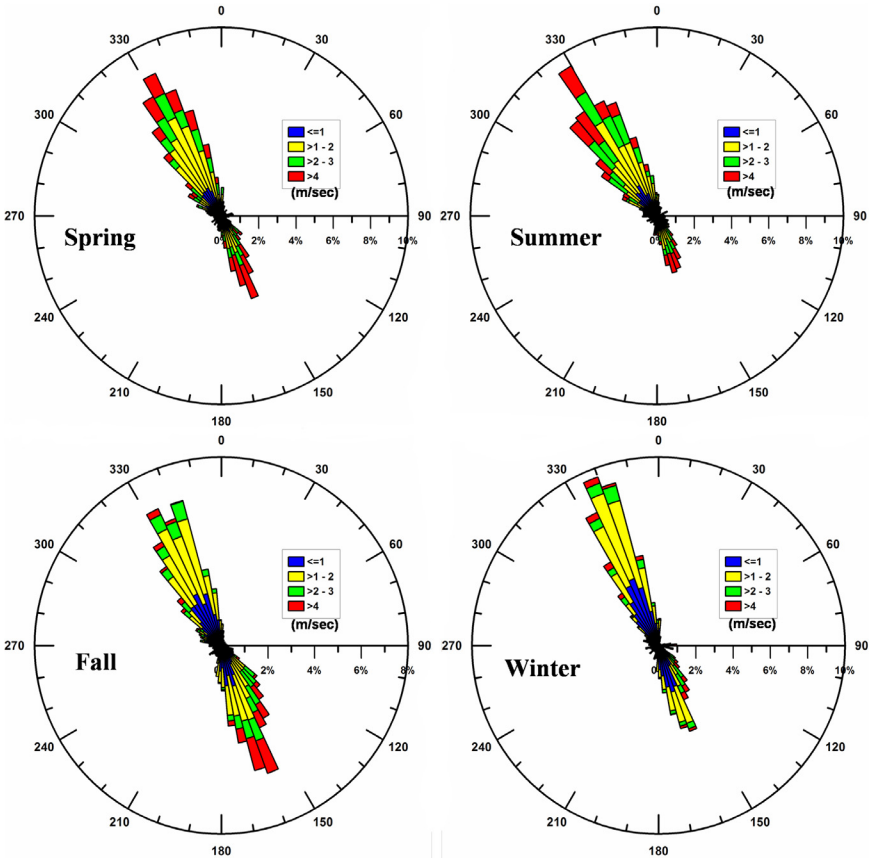

Figure 2. Seasonal wind roses for downtown Golden from November 2004 to August 2006.

2.2 Sampling and Analysis

Integrated twenty-four hour ambient aerosol samples were collected by a Partisol-Plus 2025D sequential dichot particulate sampler (Rupprecht & Pataschnick CO., Inc.) along with a Partisol 2300 speciation sampler (Rupprecht & Pataschnick CO., Inc.) using a one-in-three day schedule from November 2004 to August 2006. All collected samples were analyzed by the Analysis and Air Quality Division (AAQD) at the Environmental Technology Centre (ETC) in Ottawa, Canada. Teflon filter samples obtained by the Partisol-Plus 2025D sequential sampler were subjected to gravimetric analysis and energy dispersive X-ray Fluorescence (XRF) analysis for trace metals (Al, Sb, Ba, Br, Ca, Cd, Cr, Co, Fe, Pb, K, Mn, Ni, Rb, S, Se, Sr, Si, Sn, Ti, V, Zn).

The Partisol 2300 speciation sampler was equipped with three Harvard-designed Chemcomb cartridges which employ honeycomb-type annular denuders and filter packs consisting of a Teflon filter followed by a Nylon filter. The filters were extracted and analyzed by Ion Chromatography (IC) to quantify water-extractable anions and cations: sulphate, nitrate, ammonium, calcium, chloride, potassium, magnesium, sodium, acetic acid, formic acid, oxalic acid. The aqueous extract of $PM_{2.5}$ was also analyzed by Inductively-coupled Plasma Mass Spectrometry (ICP-MS) to quantify water-soluble species (Al, Sb, As, Ba, Be, Cd, Cr, Co, Cu, Fe, Pb, Mn, Mo, Ni, Se, Ag, Sr, Tl, Sn, Ti, V, Zn). Field blank filters were mainly taken every month and the average blank values over all blanks were used to blank correction of species concentrations in the study.

Organic carbon (OC) and elemental carbon (EC) masses were determined, based on particulate matter collected on quartz fiber filters, using a DRI Model 2001 thermal/dual-optical carbon analyzer (Atmoslytic Inc.) and the Interagency Monitoring and Protected Visual Environments (IMPROVE) analysis protocol. Quartz filter samples were heated stepwise at temperatures of 120°C (OC1), 250°C (OC2), 450°C (OC3) and 550°C (OC4) in a non-oxidizing helium (He) atmosphere, and 550°C (EC1), 700°C (EC2), and 800°C (EC3) in an oxidizing 2% O_2 / 98% He atmosphere. As temperature increased in the inert helium, some of the organic carbon pyrolized to elemental carbon, resulting in darkening of the filter deposit. The degree to which the filter was darkened was monitored by measuring the intensity of light reflected and transmitted while it was being analyzed. The light reflectance/transmittance monitored by a 632nm He-Ne laser beam through the filter was used for determining the split point between the pyrolized carbon formed from the organic carbon that was originally presented in the sample. During the oxidizing step, EC and pyrolyzed OC were combusted and the light reflectance and transmittance through the filter increased to the background levels for a clean quartz filter. Pyrolyzed organic carbon (OP) was reported as the carbon evolved from the filter after O_2 was introduced but before the reflectance/ transmittance achieved its original value. The eight fractions, OC1, OC2, OC3, OC4, EC1, EC2, EC3, and OP obtained by the reflectance method were applied for the PMF modeling in this study. Field blank corrections were also applied to these eight carbon fractions by subtracting mean carbon blank concentrations. The minimum

detection limits of total OC and EC were 0.61 μg m^{-3} and 0.14 μg m^{-3}, respectively. Since the minimum detection limit values were only available for total OC and EC, detection limits for the eight carbon fractions were calculated by dividing the total detection limit by the total number of OC and EC fractions, i.e., 0.15 μg m^{-3} for OC1 and 0.04 μg m^{-3} for EC1.

Teflon filter samples obtained by the Paritsol 2300 speciation sampler and the Partisol-Plus 2025 D sequential dichot particulate sampler were weighed before and after sample collection using a Mettler 5 microbalance (Mettler-Toledo Inc.), under controlled relative humidity and temperature conditions. The filters were stored in a controlled humidity and temperature room for 24-hr prior to weighing in order to ensure removal of particle-bound water. Laboratory quality control checks included lot stability checks, pre- and post-sampling weighing of field blanks, replicate of lab blanks and working mass standards, and replicate filter weighing. Balance verification and check of working mass standards were performed at regular intervals.

Black carbon (BC) mass was determined by optical transmissiometry. A two-wavelength Aethalometer (AE41, Magee Scientific) was used to measure the optical absorption of $PM_{2.5}$ ambient aerosol at 880 nm (AE-BC) and 370 nm (AE-UV). Wood smoke -related organic aerosol components such as certain polycyclic aromatic hydrocarbons (PAHs) tend to enhance optical absorption at 370 nm relative to 880 nm (Jenkins et al. 1996; Jeong et al. 2004). Continuous concentrations of PM_{10} and $PM_{2.5}$ measured by using a Tapered Element Oscillating Microbalance (TEOM) operated at 40°C and ambient gaseous pollutants: CO, NO_x, SO_2, and O_3, were obtained at the collocated monitoring site. The high time resolution data were applied to identify their diurnal characteristics and through correlation analysis to support the identifications of the PMF modeled factors.

Volatile organic compound samples were collected every sixth day by drawing ambient air into empty stainless steel canisters over a twenty-four hour period from May 4, 2005 to August 15, 2006. Collected gas-phase samples were analyzed using a cryogenic pre-concentration technique with a high-resolution Gas Chromatograph and quadropole Mass-selective Detector (GC-MSD). The detection limit was 0.05 μg m^{-3}. A detailed description of the analytical

methods can be found on the ETC website (http://www.etc-cte.ec.gc.ca/NAPS). A total of 153 components (122 non-polar VOCs and 31 polar VOCs) were measured in 64 samples (non-polar VOCs) and 46 samples (polar VOCs) during the measurement period. Concentrations of VOCs were compared with the contributions of resolved factors and trace gases. Fifty-seven samples of levoglucosan were collected every third day from November 8, 2004 to October 22, 2005. The levoglucosan concentration was compared with the PMF-modeled factor contributions to identify wood burning related factors. In addition to ambient pollutant data, meteorological data including ambient temperature, wind speed, and wind direction were obtained to provide insight into the influence of these parameters on source contributions at the Golden site.

2.3 Receptor modeling by PMF

In PMF, a matrix X ($n \times m$), where n is the number of samples and m is the number of chemical species is factored into two matrices, G ($n \times p$) and F ($p \times m$), where p is the number of sources, and a residual matrix E is used to account for the unapportioned part of X. The factor analysis model can be written as:

$$x_{ij} = \sum_{k=1}^{p} g_{ik} f_{kj} + e_{ij} \quad \textbf{(1)}$$

where x_{ij} is the concentration at a receptor for the j^{th} species in the i^{th} sample, g_{ik} is the particulate mass concentration from the k^{th} source contributing to the i^{th} sample, f_{kj} is the j^{th} species mass fraction from the k^{th} source, and e_{ij} is the residual between measured and modeled concentrations for the j^{th} species in the i^{th} sample. The goal of multivariate receptor modeling is to determine the number of sources (p), the source contributions (g_{ik}), and the chemical profiles (f_{kj}) of the identified sources.

The task of PMF is thus to minimize the object function (Q), defined as:

$$\mathrm{Q} = \sum_{i=1}^{n}\sum_{j=1}^{m}\left(\frac{e_{ij}}{s_{ij}}\right)^2 = \sum_{i=1}^{n}\sum_{j=1}^{m}\left(\frac{x_{ij} - \sum_{k=1}^{p} g_{ik} f_{kj}}{s_{ij}}\right)^2 \quad \textbf{(2)}$$

where s_{ij} is the user-defined uncertainty in the j^{th} species for the i^{th} sample. This factor analysis ensures that all of the species profiles (matrix F) should be non-negative and each sample must have a non-negative source contribution (matrix G). PMF is able to simultaneously change the elements of G and F in each iterative step so that Q is minimized (Paatero 1997). The Q value can be used to determine the optimal number of the factors. The theoretical Q value should be approximately equal to a value of $n \times m$, the number of values in the data matrix or the degree of freedom of the datum in the data set.

While fitting, PMF can calculate the uncertainty, s_{ij}, for x_{ij} based on its value and its associated analytical error (σ_{ij}). There are a number of models available to estimate the uncertainty (s_{ij}). In this study, the uncertainties (s_{ij}) were heuristically calculated by the error model:

$$s_{ij} = C_1 + C_3 \max\left(\left|x_{ij}\right|, \left|\sum_{k=1}^{p} g_{ik} f_{kj}\right|\right) \quad \textbf{(3)}$$

where C_1 is the analytical error (σ_{ij}) and C_3 is a dimensionless error constant chosen by trial and error, 0.05 and 0.1 in the work. The analytical errors, ranging from 10 to 35% for data above the minimum detection limit, were estimated based on routine calibration checks as well as laboratory and field blank tests by the AAQD at the ETC of Environment Canada. One of the most important advantages of PMF is that missing and below detection limit data can be included in the analysis by assigning estimates with large associated uncertainties. This feature is very useful for receptor modeling of environmental data such as that used in this study, where it is important to incorporate all available information. Missing data was established as the

median of all the concentrations measured for each species and its accompanying error (σ_{ij}) was set at four times the median value. Data below the detection limit was reflected with a concentration value equal to half of the detection limit for the given species, and the associated error (σ_{ij}) was set at 5/6 times the detection limit value (Polissar et al. 1998).

In addition, down-weighting factors were assigned to several species that exhibited much higher noise than signal based on their signal-to-noise ratio (S/N) (Paatero and Hopke 2003). In the work, the S/N ratio was defined as:

$$\mathrm{S/N} = \frac{1}{2}\sqrt{\sum_{i=1}^{n} x_i^2 \Big/ \sum_{i=1}^{n} \sigma_i^2} \qquad \textbf{(4)}$$

where x_i and σ_i are the species concentration and its analytical error in the i^{th} sample, respectively. In this work, the elements were classified into two groups; S/N < 0.5 and S/N ≥ 0.5. For the latter, weak species that had noisy variability, C_1 in eq. 3 was multiplied by three. The down-weighting for weak variables was useful for minimizing the impact of the noisy variables in the PMF analysis.

Although the imposition of non-negativity constraints on the factors decreases the degree of rotational freedom and helps to identify unique solutions, some rotational ambiguity generally remains in the PMF analysis (Paatero et al. 2002). The rotational ambiguity can be effectively reduced and more physically realistic solutions are produced by trial and error using the user-defined parameter FPEAK in PMF (Paatero 1998). By setting a positive value of FPEAK the PMF model is forced to subtract the source profiles from each other to yield a more plausible solution.

EPA PMF (ver. 1.1) allows source contributions to be slightly negative and currently provides no options for the minimization of rotational ambiguity such as the FPEAK parameter. The EPA PMF is presented in more detail by Eberly (2005). Uncertainties in the source compositions were estimated by a bootstrap procedure to perform the analysis on random subsamples of the data. The statistical method, bootstrap, is typically used to estimate quantities associated with

the sampling distribution of estimators and test statistics (Efron and Tibshirani 1993). In this work, the data was resampled more than 500 times with replacement. For each resampling, the model was run and a new source composition was calculated. The standard deviation of these resampled results was the estimate of the standard error, and the 2.5 and 97.5 percentiles of the distribution of the statistics were used to estimate the bounds of 95% confidence intervals.

2.4 Wind Sector Analysis

Conditional Probability Function (CPF) analysis was applied to the resolved source contributions to determine the likely direction of each source from the receptor site. CPF evaluates the probability that a source is located within a particular wind direction sector. The CPF is defined as follows:

$$CPF = \frac{m_{\Delta\theta}}{n_{\Delta\theta}} \quad \textbf{(5)}$$

where $m_{\Delta\theta}$ is the number of times that the source contribution exceeded a certain threshold criteria while wind came from a direction sector ($\Delta\theta$) and $n_{\Delta\theta}$ is the total number of times the wind came from the same wind direction (Ashbaugh 1985). In this study, the direction sector ($\Delta\theta$) was set to be 10 degrees. Hourly wind direction data was converted to daily averaged data by using a vector average method indicating change of wind direction with the intensity of wind speed. All time periods of wind speed less than 1 m/sec were removed from the analysis (30 samples of 174 samples). The threshold was set as the highest 25% of the source contribution concentrations.

3. RESULTS AND DISCUSSION

3.1 Selection of Species

Inclusion and exclusion of species can significantly influence the PMF model results. In this study, species with less than 10% of data available and more than 80% of data below the minimum detection limit were excluded from the PMF modeling. Multiple analyses were provided for the elements : Al, Ba, Ca, Cr, Fe, K, Mn, Pb, Sr, and Zn by overlap between XRF and ICP-MS (or IC) methods. Sulphate and sulphur were measured using IC and XRF, respectively. Table 1 shows the data availability and signal-to-noise (S/N) ratios of the elements. Chemical components with significantly higher data completeness (two times higher percentage of valid data) were included in the PMF analysis, as shown in the Table 1. For the remaining species, Ba, Ca, Cr, Fe, K, Mn, and Zn, elements with higher S/N ratios, indicating better resolved variability, were chosen.

Linear correlation coefficients (r^2) between Ca, Fe, K, S, and sulphate measured by two independent analytical methods were examined to evaluate data consistency (Figure 3). The data for soluble Ca ion and Ca from XRF were found to be in good agreements. The linear relationship between the two exhibited a coefficient of determination of 0.79 (sample number, n=108). The ratio of Ca by XRF to soluble Ca by IC ranged from 0.2 to 5.1 over the entire sampling period with a mean of 0.9. The good agreement indicated there was no advantage to incorporating both the soluble Ca and total Ca into the PMF analysis. The ratio of total potassium by XRF to water-soluble potassium by IC ranged from 0.8 to 10.1 with a moderate correlation during the study period (r^2=0.60, n=80). Soluble K by IC is known as a marker of biomass burning while insoluble K is most likely related to crustal material (Andreae 1983; Ma et al. 2003). The correlation between Fe values measured by XRF and ICP-MS was relatively low (r^2=0.52, n=115). Although most of the Fe concentrations were above the detection limit, the analytical uncertainties of the Fe measurements by the two methods tended to be higher than other element analyses. Due to 1/3 molecular weight (M.W.), sulphate (M.W. = 96) concentrations should be about three times the sulfur (M.W. = 32) concentration. The

comparison of sulphate by IC and total sulfur by XRF showed a good agreement with a ratio of 2.94 ± 1.16 (n=127). In this study, sulphate by IC was chosen as the variable for the PMF analysis because of its high S/N ratio.

Table 1. Data availability and signal-to-noise ratios of collocated species.

Species	Methods	*Valid (%)	*BDL (%)	*Missing (%)	*S/N
Al	**XRF**	**72**	**5**	**23**	**0.46**
	ICP-MS	33	27	40	0.47
Ba	XRF	60	17	23	0.29
	ICP-MS	**91**	**1**	**8**	**0.56**
Ca	XRF	74	3	23	0.65
	****IC**	**85**	**13**	**2**	**2.07**
Cr	XRF	18	59	23	0.35
	ICP-MS	**27**	**65**	**8**	**0.97**
Fe	**XRF**	**76**	**0**	**24**	**0.34**
	ICP-MS	90	2	8	0.20
K	XRF	75	2	23	0.38
	IC	**60**	**37**	**2**	**1.67**
Mn	XRF	18	59	23	0.38
	ICP-MS	**91**	**1**	**8**	**0.59**
Pb	XRF	13	64	23	0.24
	ICP-MS	**86**	**6**	**9**	**0.59**
Sr	XRF	10	67	23	0.30
	ICP-MS	**61**	**30**	**9**	**0.76**
Zn	XRF	48	29	23	0.49
	ICP-MS	**66**	**26**	**9**	**0.73**
Sulphur	XRF	76	1	23	0.37
Sulphate	**IC**	**98**	**0**	**2**	**1.29**

Selected analytical techniques were shown in bold.
* Valid : data above the detection limit, BDL: data below the detection limit, Missing : missing data, S/N: signal-to-noise ratio.
** water soluble ions

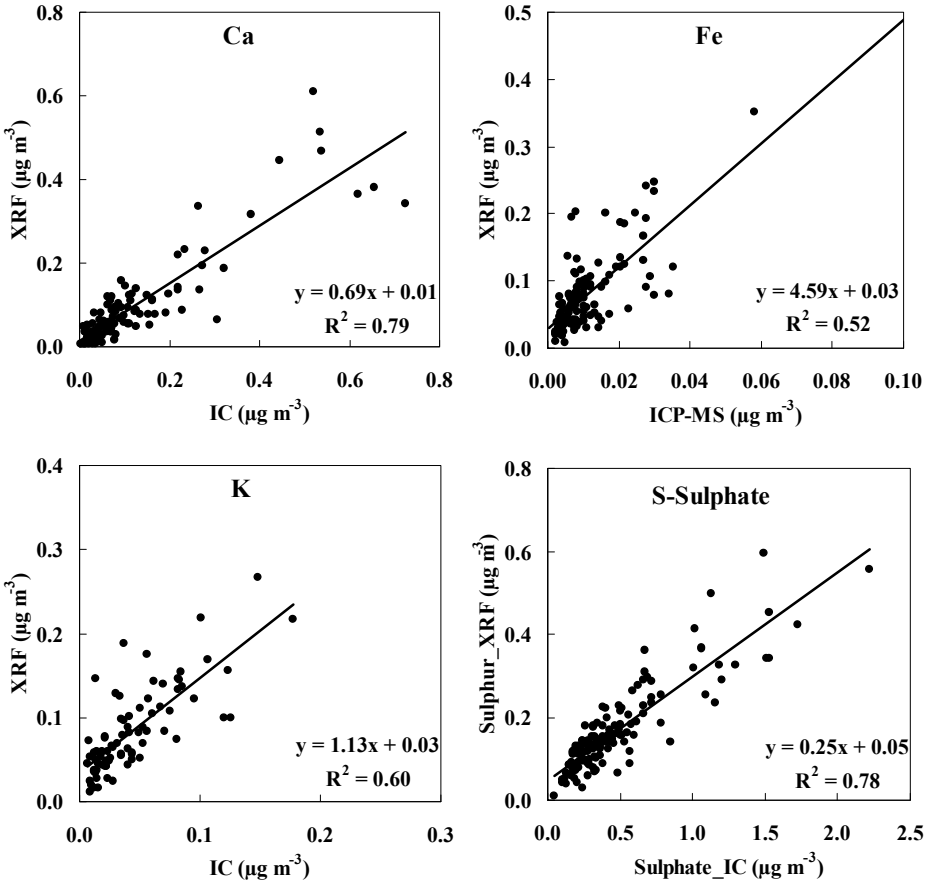

Figure 3. Inter-comparisons of selected species concentrations measured by XRF, IC, and ICP-MS methods.

3.2 Identification of Unusual Data

Data validation tests to identify values that appeared abnormal as compared to the overall data were carefully performed using scatter plot and time series analysis. At the Golden site, an extremely high concentration of strontium was observed on October 31(Halloween day), 2005 (Figure 4). Noticeably high concentrations of K and Pb were also observed on the event day, suggesting a local burning/fireworks event. All species measured on the event day were excluded from the source apportionment since unique events tend to be separated into their own factors in the PMF analysis. In order to avoid unrealistic source apportionment and to minimize the impact of a single episodic occurrence exhibiting a unique profile, a total of seventeen datum

were identified as outliers and were excluded by representing them as missing values.

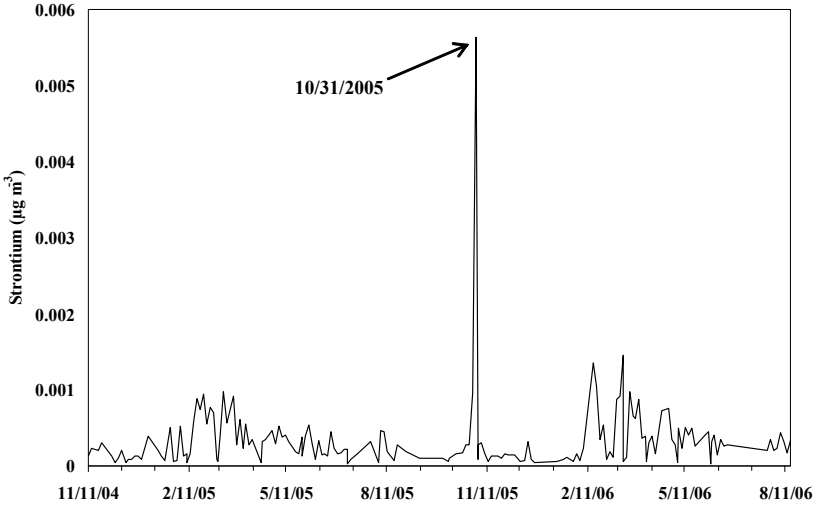

Figure 4. Time-series plot of daily (every third day) strontium concentrations in Golden.

Table 2 presents a statistical summary of the selected species for the PMF modeling. To estimate these summary statistics, all missing data values were excluded and data below the detection limit were substituted by one half of the detection limit for each species, as described in the method section.

Table 2. Descriptive statistics and signal-to-noise ratios for the data selected for use in the PMF analysis at the Golden site.

Species	Analytical Method	Average ($\mu g\ m^{-3}$)	Median ($\mu g\ m^{-3}$)	StDev ($\mu g\ m^{-3}$)	Min ($\mu g\ m^{-3}$)	Max ($\mu g\ m^{-3}$)	Valid (%)	BDL (%)	Missing (%)	S/N
Acetate	IC	2.73E-02	5.22E-03	3.59E-02	5.20E-03	1.92E-01	40	58	2	1.16
Ammonium	IC	2.23E-01	1.66E-01	1.96E-01	2.09E-03	1.17E+00	97	1	2	1.40
Ca	IC	9.78E-02	5.77E-02	1.28E-01	1.04E-03	7.24E-01	85	13	2	2.07
Formate	IC	3.02E-02	2.72E-02	2.44E-02	5.21E-03	1.61E-01	68	30	2	1.03
Mg	IC	9.84E-03	7.46E-03	9.18E-03	1.04E-03	4.89E-02	75	22	2	1.39
Oxalate	IC	4.73E-02	4.79E-02	2.76E-02	5.21E-03	1.41E-01	82	16	2	0.95
K	IC	2.70E-02	1.44E-02	3.23E-02	3.12E-03	1.77E-01	60	37	2	1.67
Na	IC	5.98E-02	2.40E-02	1.88E-01	1.74E-03	2.18E+00	66	30	3	2.62
Cl	IC	4.90E-02	1.64E-02	6.74E-02	1.35E-02	4.28E-01	36	61	2	1.58
Nitrate	IC	3.48E-01	2.20E-01	3.78E-01	1.32E-02	2.74E+00	87	11	2	1.78
Sulphate	IC	4.98E-01	3.73E-01	3.70E-01	3.09E-02	2.15E+00	98	0	2	1.29
Sb	ICP-MS	3.97E-05	2.09E-05	4.60E-05	1.87E-05	4.10E-04	29	63	8	0.69
As	ICP-MS	1.04E-04	7.60E-05	6.92E-05	1.56E-05	3.98E-04	58	31	11	0.46
Ba	ICP-MS	1.30E-03	1.19E-03	7.96E-04	7.93E-05	5.49E-03	91	1	8	0.56
Cd	ICP-MS	3.63E-05	2.98E-05	2.67E-05	1.04E-05	1.16E-04	57	33	10	0.47
Cr	ICP-MS	1.25E-04	6.96E-05	9.30E-05	6.93E-05	5.63E-04	25	65	10	0.60
Cu	ICP-MS	2.85E-04	2.09E-04	2.95E-04	9.47E-05	1.94E-03	39	51	10	0.64
Pb	ICP-MS	2.88E-04	2.51E-04	2.06E-04	2.43E-05	1.22E-03	86	6	9	0.59
Mn	ICP-MS	9.12E-04	7.92E-04	5.90E-04	4.69E-05	3.02E-03	91	1	8	0.59
Ni	ICP-MS	6.51E-05	4.54E-05	6.39E-05	3.13E-05	5.24E-04	18	74	8	0.60
Sr	ICP-MS	2.70E-04	1.95E-04	2.62E-04	3.47E-05	1.41E-03	61	30	9	0.76
V	ICP-MS	2.98E-05	2.09E-05	1.55E-05	2.08E-05	9.06E-05	13	79	8	0.41
Zn	ICP-MS	7.48E-03	3.61E-03	6.96E-03	3.60E-03	4.65E-02	32	59	9	0.60
Al	XRF	5.41E-02	3.69E-02	5.50E-02	6.20E-04	3.17E-01	72	5	23	0.46
Fe	XRF	8.26E-02	7.17E-02	5.95E-02	7.87E-03	3.51E-01	76	0	24	0.34
Si	XRF	1.20E-01	9.17E-02	1.18E-01	6.20E-04	8.59E-01	73	4	23	0.45
Ti	XRF	1.20E-02	8.16E-03	8.49E-03	4.53E-04	4.44E-02	20	57	23	0.34
OC1	IMPROVE	8.39E-01	3.20E-01	1.30E+00	7.67E-02	7.97E+00	63	30	7	1.99
OC2	IMPROVE	1.83E+00	1.37E+00	1.31E+00	7.70E-02	6.24E+00	93	1	7	0.76
OC3	IMPROVE	2.03E+00	1.66E+00	1.15E+00	2.71E-01	5.13E+00	93	0	7	0.65
OC4	IMPROVE	1.09E+00	9.78E-01	5.69E-01	1.71E-01	2.91E+00	93	0	7	0.59
OP	IMPROVE	9.11E-01	7.47E-01	7.01E-01	7.70E-02	3.06E+00	84	9	7	0.71
EC1	IMPROVE	1.80E+00	1.32E+00	1.50E+00	9.43E-02	6.81E+00	93	0	7	0.80
EC2	IMPROVE	6.60E-01	5.45E-01	4.20E-01	8.09E-02	2.06E+00	93	0	7	0.66
EC3	IMPROVE	5.53E-02	1.77E-02	5.02E-02	1.77E-02	2.23E-01	44	49	7	0.76

Valid : data above the detection limit, BDL: data below the minimum detection limit, Missing : missing data

3.3 Mass Closure of $PM_{2.5}$

As shown in Figure 5, the sum of the species concentrations plotted against the total $PM_{2.5}$ mass as measured by the R&P Partisol-Plus 2025 D sequential dichot particulate sampler and the R&P Partisol 2300 speciation sampler showed an excellent correlation. Twenty-four hour integrated data from the two $PM_{2.5}$ mass measurement methods agreed well with a linear regression r^2 value of 0.89, slope of 0.96, and intercept of 0.16. Note that total $PM_{2.5}$ mass levels measured on June 1 to 16, 2006 by the Partisol 2300 sampler were excluded since the data were abnormally high, as compared to the $PM_{2.5}$ mass values by the Partisol-Plus 2025D as well as the sum of the species concentrations. In order to estimate the sum of the species, concentrations of organic acids, acetate, formate, and oxalate, were excluded to avoid double counting this organic matter mass. In addition, the ratio of oxygen to carbon in organic PM was assumed to be 1.3, slightly below the typical mass of organic PM (OM) factor of 1.4 often used for the western United States. Using a value of 1.4 resulted in the sum of the species components overestimating to total measured mass. In the PMF modeling, the total $PM_{2.5}$ mass concentrations by the Partisol 2300 sampler were used for the conversion of PMF-resolved factor contributions to meaningful mass concentrations due to the high data availability and reliability of the sampler.

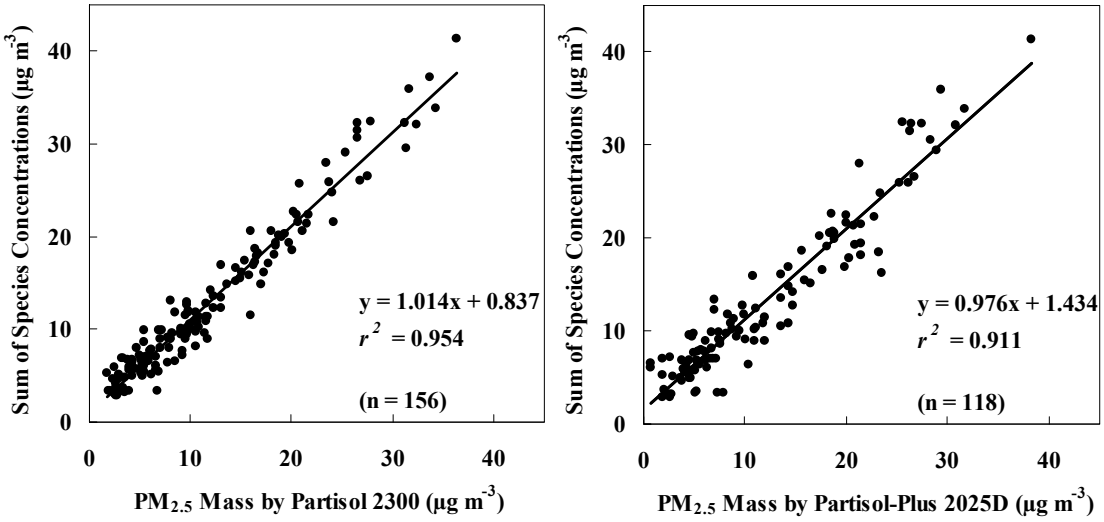

Figure 5. Comparison of sum of species concentrations and $PM_{2.5}$ mass concentration measured by the R&P Partisol 2300 and the R&P Partisol-Plus 2025D.

3.4 Temporal Characteristics of Species Concentrations

The average concentration and the 98th percentile value of the total $PM_{2.5}$ measured by the Partisol 2300 sampler over the entire sampling period were 11.5 ± 7.8 μg m^{-3} (mean ± standard deviation) and 32.1 μg m^{-3}, respectively. The highest $PM_{2.5}$ mass was observed in winter months (December - February) with an average of 18.0 ± 9.1 μg m^{-3}, whereas the lowest value was typically found in summer months (June - August) with an average of 6.1 ± 3.3 μg m^{-3}. The average concentration of $PM_{2.5}$ from December 2004 to February 2005 was approximately 22% higher than the value from December 2005 to February 2006. However, the average $PM_{2.5}$ mass from June to August 2005 was lower than the average from June to August 2006 by a factor of 1.5 at the Golden site.

Seasonal variations in $PM_{2.5}$ chemical components and their contributions to the total $PM_{2.5}$ mass are shown in Figure 6. The average concentration of $PM_{2.5}$ in winter was significantly higher than the concentration in summer by a ratio of approximately three during the measurement period. The mass contributions of major species, total OC (sum of OC1, OC2, OC3, OC4, and OP), total EC (sum of EC1, EC2, and EC3 subtracted by OP), nitrate, sulphate, and ammonium as well as minor trace elements indicated that carbonaceous compounds, total OC and EC, were the largest contributors to the $PM_{2.5}$ mass in all seasons. It should be noted that the organic carbon fractions have not been converted to organic mass, to account for oxygen content. As a result, the sum of all the compounds accounted for less than 100% of the $PM_{2.5}$ Mass. The increased OC and EC in winter could be explained by meteorological changes such as low mixing boundary layers with frequent temperature inversions in winter as well as an increased emission rate of certain sources: residential heating/wood burning in particular. Average winter to summer concentration ratios of the eight carbonaceous components of $PM_{2.5}$ were about 12.7 (OC1), 3.3 (OC2), 3.0 (OC3), 2.8 (OC4), 5.3 (OP), 6.5 (EC1), 1.4 (EC2), and 0.8 (EC3) over the sampling period. The carbon components with apparently high ratios (much higher than the average ratio of 4.5) can be considered as markers that are strongly related to sources with significant seasonal variations producing increases beyond that due to meteorological changes alone. The high winter/summer ratio suggests that OC1, the most volatile organic carbon

fraction, was probably secondary organic carbon contributed by anthropogenic winter activities. On average, EC1 concentration in the summer was significantly lower than the level in the winter by a factor of six, whereas EC2 concentration was slightly lower in the summer than in the winter in spite of generally high mixing heights in the summer. The low seasonal variation of EC2 implies that the source contribution of EC2 increased in summer in contrast to other EC fractions. Figure 6 also depicts seasonality in the nitrate concentrations, consistent with typical increased nitrate formation in winter, whereas the seasonal changes in sulphate concentrations did not show any apparent distinctions between the summer and winter concentrations. On average, sulphate concentrations were found to be lower in the summer than in the winter or spring. Strong seasonality in the concentrations of Si, Ca, and Al, typical markers for soil components, was observed in spring (March-May). The highest concentration of sodium was found in spring as well, probably indicating the detection of re-suspended road salt. The Fe and oxalic acid (oxalate) concentrations increased in summer by factors of 1.4 and 1.9, respectively, as compared to the values in spring. There are possible indirect sources of oxalate, through photochemical production from ozonolysis of anthropogenic alkenes or natural alkenes. Although the formation mechanism and the precursors of oxalate have not been well identified, photochemical production in-cloud has been proposed as its major production pathway (Crahan et al. 2004). Variation in the formation of oxalate is likely dependent on the temperature and the presence of water vapor, resulting in the increased contribution of the oxalate concentration to the total $PM_{2.5}$ mass in summer.

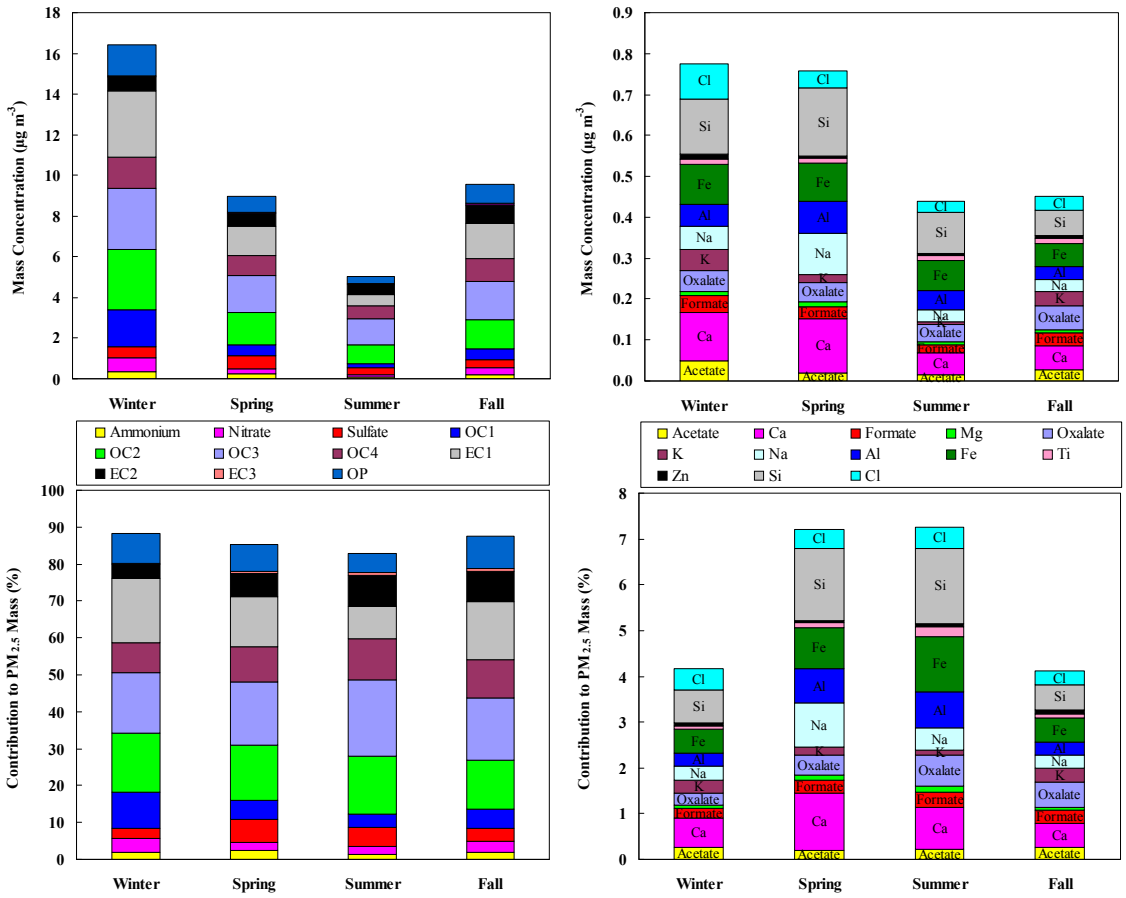

Figure 6. Seasonal variations in $PM_{2.5}$ chemical species (upper) and contributions to the total $PM_{2.5}$ mass (bottom) in Golden. Major $PM_{2.5}$ components are shown on the left; minor components are shown on the right.

3.5 Diurnal Variations in Gaseous Pollutants and Black Carbon

In order to better interpret and understand the source apportionment results, diurnal patterns in hourly averaged concentrations of ambient pollutants including gaseous species and continuous PM mass data were examined (Figure 7). The diurnal trends in summer and winter as well as on weekends and weekdays (workdays) are illustrated. In general, with the exception of ozone and PM_{10}, gaseous pollutants and continuous $PM_{2.5}$ mass were higher in the winter than in the summer. This could be due to an increase in the source contributions as well as reduced dilution caused by low mixing heights and temperature inversion events, which frequently occurred

throughout the winter in this valley area. The diurnal trends in NO and SO_2 were in quite good agreement during summer and winter months although the SO_2 levels were very low, indicating the influence of common sources. In general, no distinctive differences between weekend and weekday diurnal trends exhibited in summer; however, moderate diurnal trends with a peak at around 6 a.m. (local time) were found in the concentrations of SO_2, NO and BC. Typically strong diurnal patterns with a sharp peak in the morning (8 a.m.) and a second rise in concentration starting in the late afternoon were observed in winter. In contrast to the weekend/weekday difference in the summer, the morning peak on weekdays tended to be higher than the peak on weekends in the winter, possibly caused by increased traffic sources. Anecdotal information suggest that significant numbers of trucks stop for the night in Golden and then restart their engines in the morning. In this regard, it would be worthwhile to examine diurnal fluctuations in the concentrations of ultrafine particles in Golden during the winter. The concentrations of AE-UV, BC, CO, NO, NO_2, and total $PM_{2.5}$ mass significantly increased during the evening in winter months, indicating the impact of residential heating/wood burning with reduced mixing heights. The diurnal fluctuation in the winter time mixing height likely also strongly influenced the observed diurnal trends in the winter time pollutant concentrations, causing lower midday concentrations as a results of greater mixing.

The number of motor vehicles passing Highway 1/east of Highway 95 in Golden was counted from December 2004 to November 2005. Temporal trends in vehicle numbers are shown in Figure 8. Higher numbers of vehicles were observed in summer especially in July and August, probably due to increased motor vehicle traffic during the typical vacation season. Interestingly, the diurnal pattern in the vehicle counting shows that the number of vehicles on weekends was higher than the number on weekdays in summer, whereas the vehicle number in winter showed the opposite trend. The traffic trends between summer and winter would explain the seasonal differences in the weekday/weekend effect for gaseous pollutant concentrations. No significant weekday/weekend on diurnal trends were found when the train count data for the period November, 2004 to February, 2005 was examined.

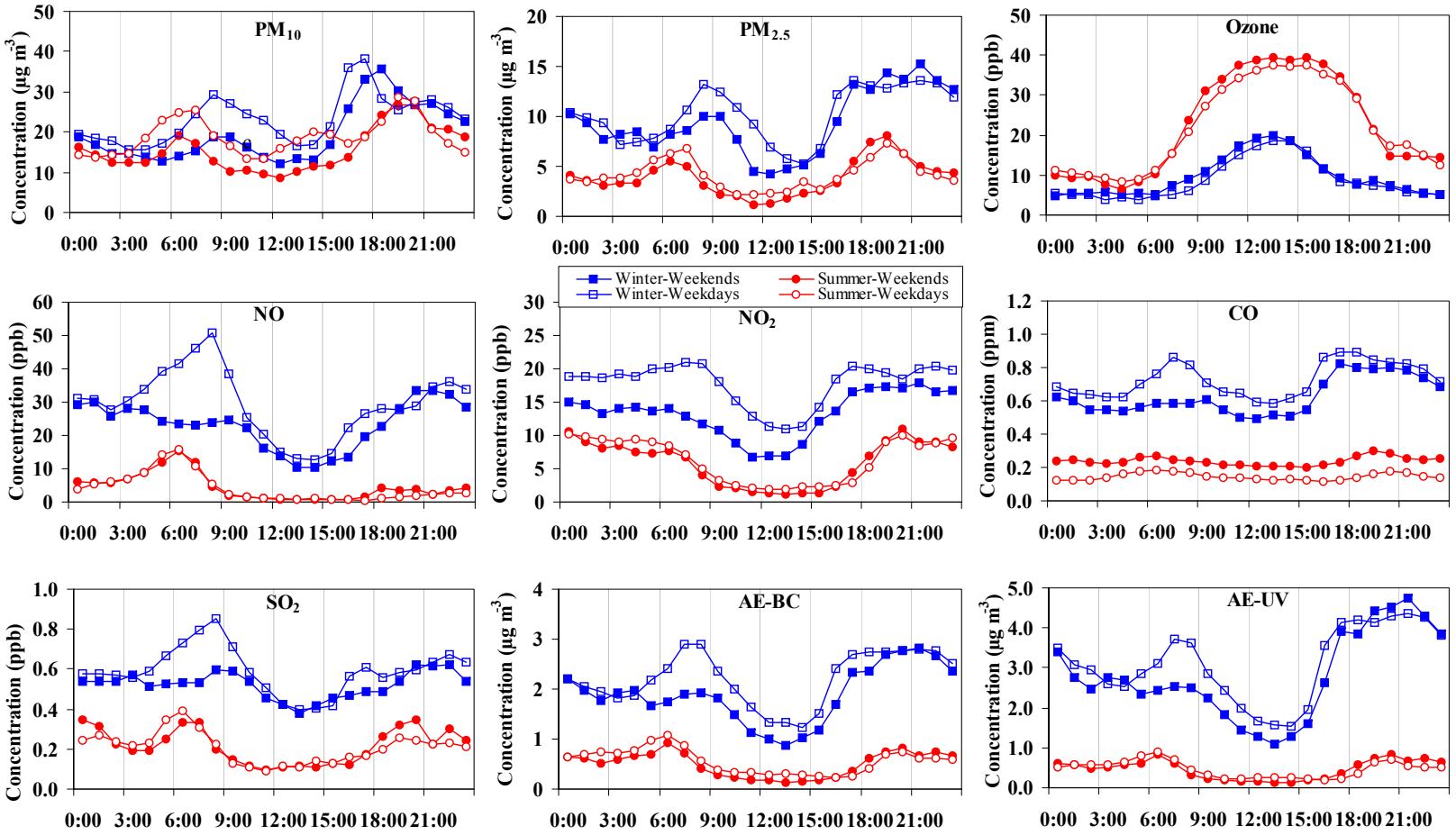

Figure 7. Diurnal variations in hourly averaged concentrations of gaseous pollutants, PM_{10}, $PM_{2.5}$ by the TEOM, and black carbon (AE-BC), UV-absorbing BC (AE-UV) by the Aethalometer from November 2005 to July 2006 at the Golden site.

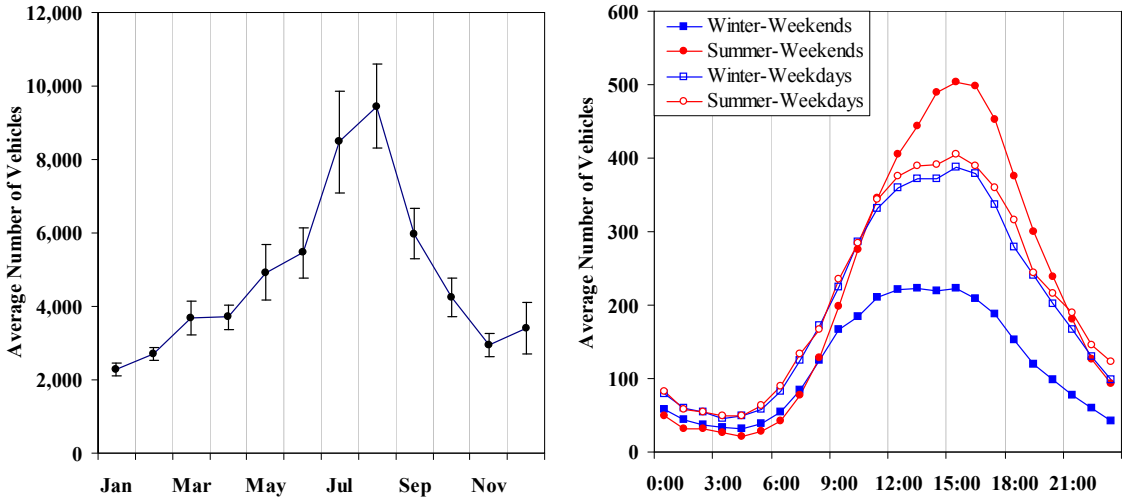

Figure 8. Seasonal and diurnal variations in the number of vehicles from December 4, 2004 to November 30, 2005 in Golden. The error bars represent the standard deviations.

3.6 PMF Analysis on Speciated $PM_{2.5}$ Data

3.6.1 PMF Model Diagnostics

Q value Analysis

PMF was applied on the data set consisting of 35 species and 174 samples collected from November 11, 2005 to August 15, 2006 in Golden, B.C. Canada. The model was run in the default robust mode to decrease the influence of extreme values on the PMF solution. It was also necessary to test different sets of error estimates to find the optimal number of solutions with a realistic physical meaning. In order to determine the optimal number of sources, different numbers of sources were explored by applying a trial and error method. For the final analysis, PMF was applied to the data set using 4 to 15 factors and the resultant change in the Q values was examined. Theoretically, the Q value should approximate the number of data in the original data set if the measurement uncertainties are reasonably estimated. In the study, the theoretical Q value was approximated to be 6090 (i.e., 174×35); however, this value was decreased due to several heavily downweighted species and the strength of an error constant. Figure 9 shows the

variations of the Q values with the number of source factors and runs when the error constant (C_3) was set at 10%. Robust Q value was the value for which the impact of outliers was minimized, while true Q value was the value for which the influence of extreme values was not controlled. As shown, the robust Q values were very close to the true Q values, implying that the model fit the outliers reasonably. It is also important that the range of Q values from random runs (100 runs in the study) should be adequately small to confirm the achievement of a similar global minimum, and hence outliers are fitted equally well for each random run. In a seven-factor solution, more than 97% of Q values were quite close to 5696 at the 5 % of the constant, and 3763 at the 10% of the error constant, showing that the Q value was the global minimum value. Based on the evaluation of the model results and the Q value variations for models, the seven-factor solution provided the most feasible results.

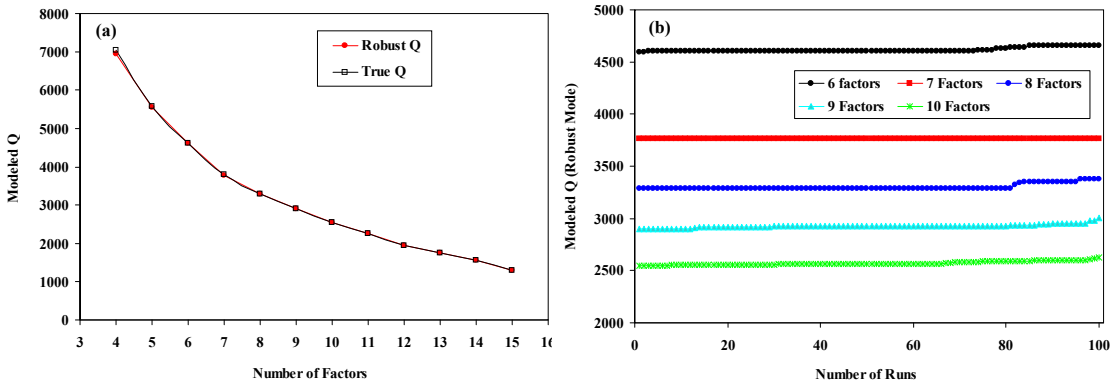

Figure 9. Variations in the Q values as a function of the number of factors (a) and runs of the model (b). The error constant was set at 10%.

Scaled Residual Analysis

To ensure that the appropriate number of factors was chosen, the scaled residuals, the ratio of the PMF-modeled residual (e_{ij}) to the input uncertainty (s_{ij}) were also examined. The distributions of scaled residuals of selected species in the seven factor PMF solution are presented in Figure 10. A reasonable solution should have scaled residuals distributed mostly between -3 and +3. On average, approximately 94% and 97% of the scaled residuals estimated by PMF were distributed

between -2 and + 2 with the error constants of 5 and 10%, respectively. As a result, a good fit of the seven-factor modeled results was identified.

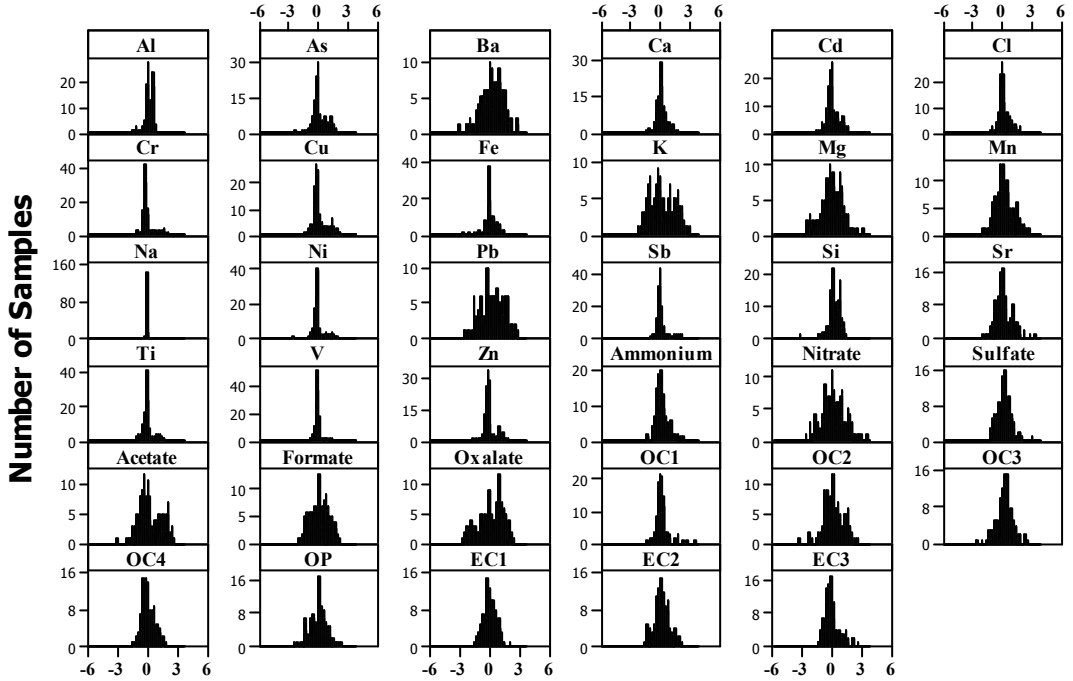

Figure 10. Histograms of the scaled residuals for 35 chemical components.

G-space Plot Analysis

G-space plotting created by scatter plots of identified sources provides useful information towards finding an optimal solution with realistic rotations. The G-space plots (Figure 11) for the 7 factors showed reasonably good edges in that they were lying on or near the x and y axes for all scatter plots. This indicates that the factors were not correlated with each other and hence that they represented distinctive sources. Note that for the G-space plots, two episodes on March 23, 2005 and March 6, 2006 of the F1 in the Figure 11 were excluded in the work.

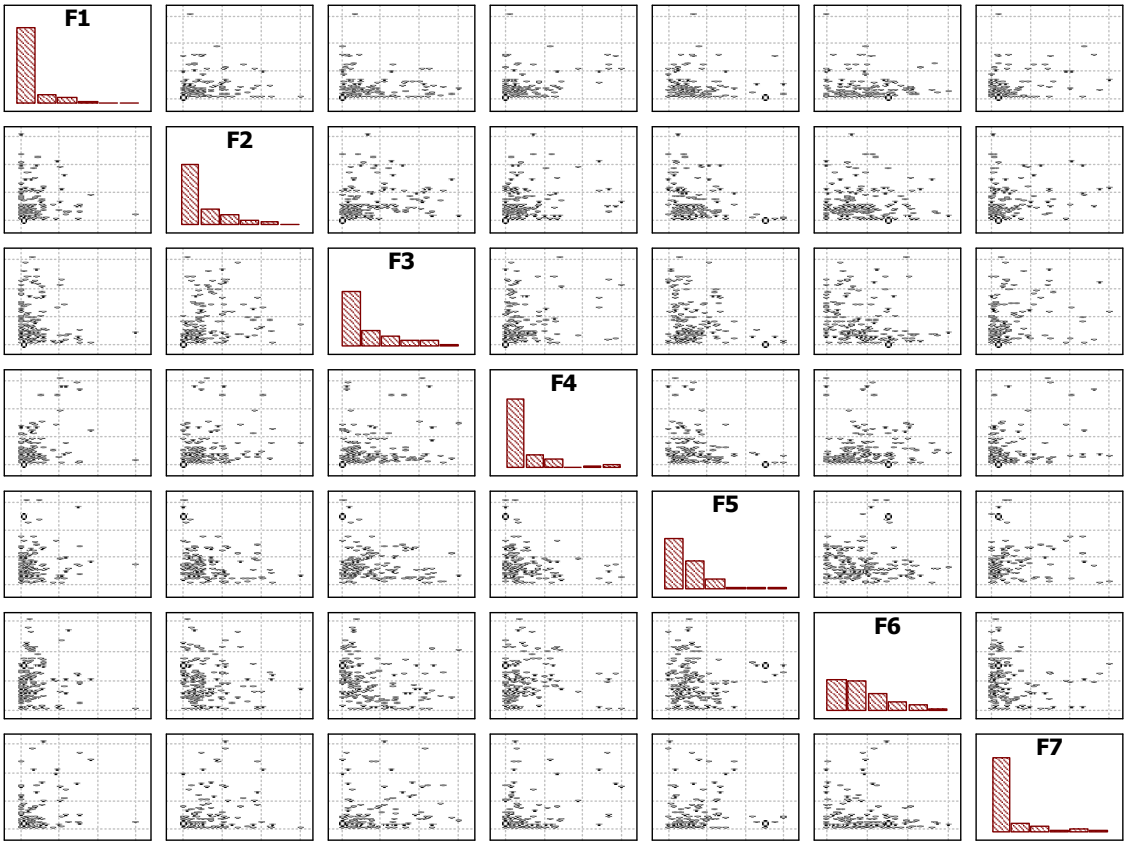

Figure 11. Edge plots for the PMF-modeled 7 factors, F1 to F7 in Golden.

3.6.2 Seven Factor Solution

The best solution was found to be the seven-factor solution for the elemental composition of the fine particulate matter in the Golden area. In Figure 12, a comparison of the reconstructed $PM_{2.5}$ contributions from all sources with measured $PM_{2.5}$ concentrations shows that the PMF resolved sources effectively reproduce the measured total mass. In addition, the PMF derived for most of the variation in the $PM_{2.5}$ concentrations with a high linear correlation coefficient (r^2 =0.945). Figure 13 presents the profiles (value ± standard deviation) of the seven sources identified; road salt, sulphate, wood burning, crustal material, traffic, wood processing, and winter heating. The temporal source contributions of these seven sources are depicted in Figure 14. The seasonal contributions of each source to the $PM_{2.5}$ mass concentrations are also shown in Figure 15. PMF

source identification was based on the presence of marker elements (e.g., K for wood burning combustion) as well as the ratio of the elements in the source profile. The correlation analyses between the time series of the contributions of sources and ambient pollutant concentrations such as molecular organics (levoglucosan, VOCs), continuous measurements of ambient pollutants, meteorological data, and the temporal variations of expected PM sources (i.e., daily traffic density) were also useful for the source identification (Tables 3 and 4). PMF analysis was conducted by varying the rotational parameter, FPEAK from -0.4 to +0.4. However, a change in rotation was not found to improve the results and the value of FPEAK was finally set equal to zero in this work. In order to determine the source contribution to $PM_{2.5}$, multiple linear regression was performed to fit the total $PM_{2.5}$ mass concentrations measured by the Partisol 2300 sampler against the modeled factor contributions. The modeled source profiles (F factor) and contributions (G factor) were normalized by the regression coefficients to convert the factor profiles and contributions into values with physically meaningful units, $\mu g\ \mu g^{-3}$ for the factor profiles and $\mu g\ m^{-3}$ for the source contributions.

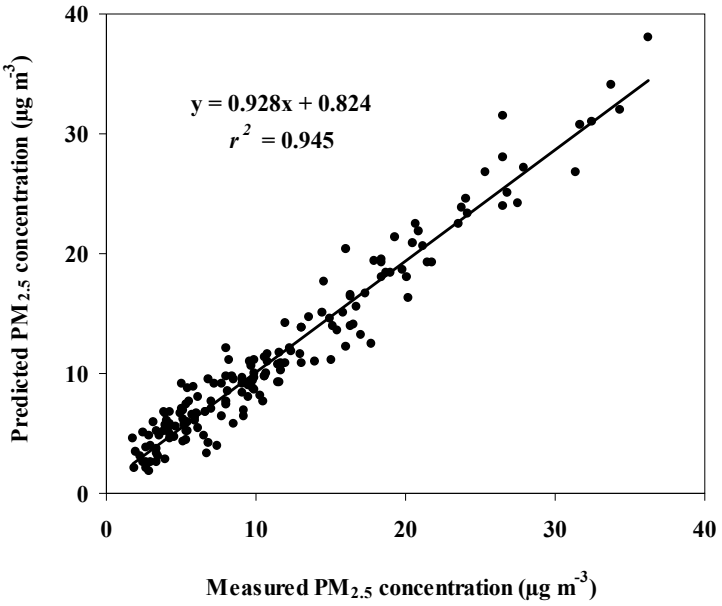

Figure 12. Measured $PM_{2.5}$ mass concentrations versus the PMF modeled $PM_{2.5}$ mass concentrations.

Road Salt Factor (F1)

The salt factor profile (F1), mainly characterized by Na and Cl ions in the factor profile, contributed 0.7 % (0.1 ± 0.2 µg m^{-3}) to the total $PM_{2.5}$ on average. Thirty percent of the Ti mass was also explained by this factor. The high concentration of Na, Cl, and Ti in the factor indicated that the salt factor could be attributed to the resuspension of salt used for deicing agents. As shown in the time series plot for the road salt source, the road salt factor achieved its highest source contribution on March 23, 2005 and March 6, 2006. According to the climate data collected by Environment Canada, snow covered the ground on March 20, 2005 and March 5, 2006 in Golden and the days of March 23, 2005 and March 6, 2006 were warm and very clear (Environment Canada 2005a). The meteorological record probably supports that the salt factor was associated with the resuspension of dried road salt particles. The contribution of the road salt factor was generally quite low except for March and April where it contributed a maximum of 1.2 % to the $PM_{2.5}$ mass.

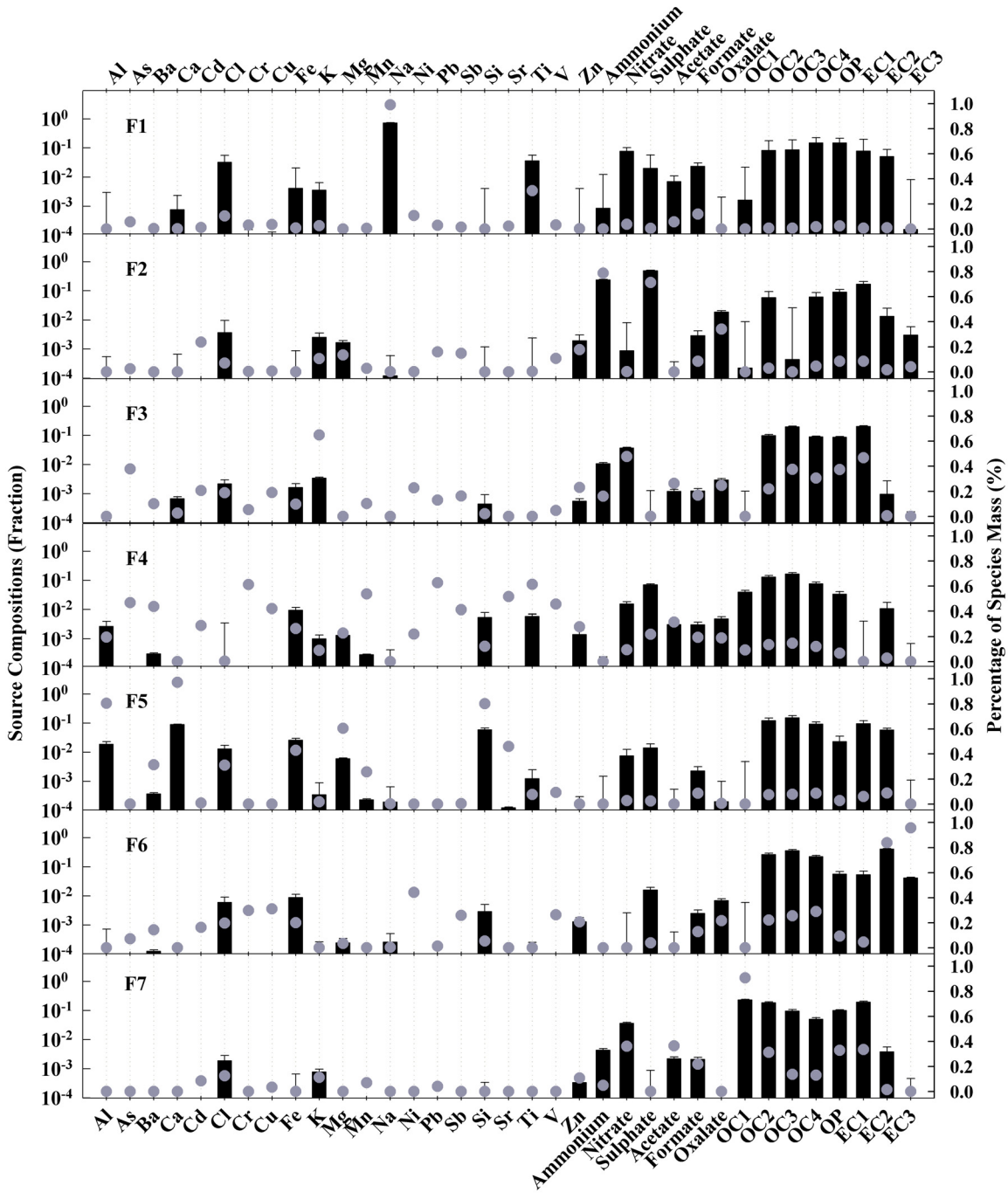

Figure 13. Source profiles for the PMF resolved seven factors ; F1: road salt, F2: sulphate , F3: wood burning, F4: wood processing, F5: crustal material, F6: traffic, and F7: winter heating in Golden. The solid bars represent the amount of each species apportioned to the factor and the dots represent the percentage of species apportioned to the factor.

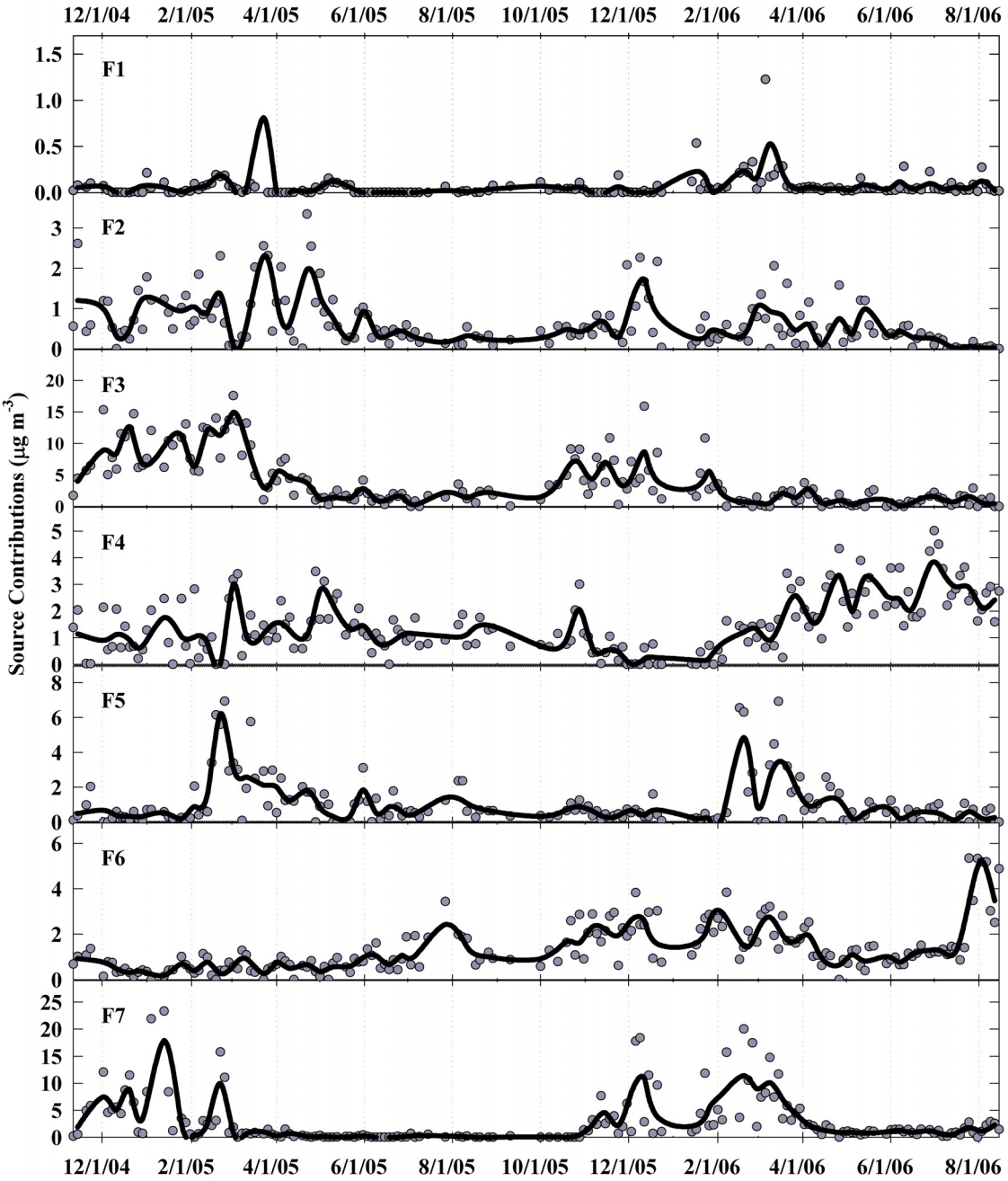

Figure 14. Source contributions for the PMF resolved seven factors; F1: road salt, F2: sulphate, F3: wood burning, F4: wood processing, F5: crustal material, F6: traffic, and F7: winter heating in Golden. Solid represents trend line as two point moving average.

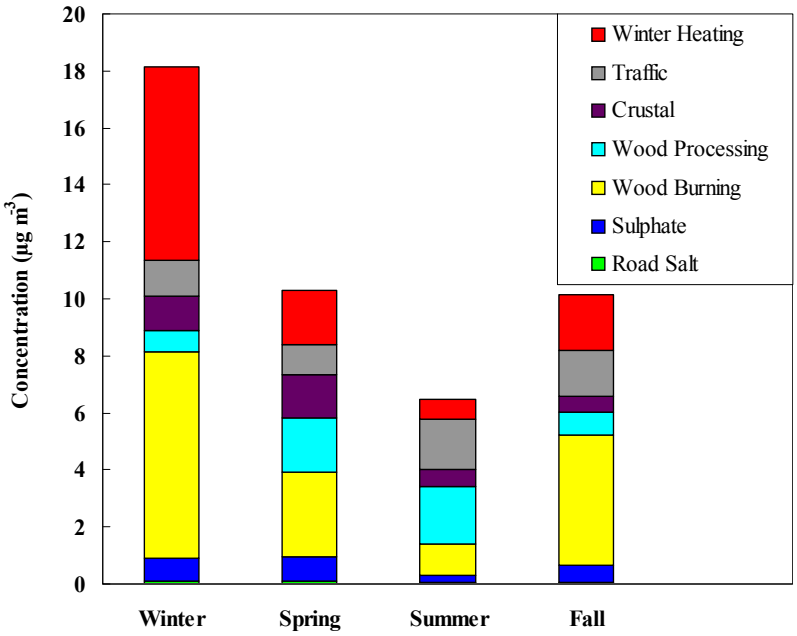

Figure 15. Seasonal variations in the contributions of the PMF-modeled seven factors in Golden.

Sulphate Factor (F2)

The resolved sulphate factor contributed 5.6 % (0.6 ± 0.6 µg m^{-3}) to the $PM_{2.5}$ mass on average. The factor accounts for 71% and 79% of the total sulphate and ammonium concentrations, respectively. Interestingly, the secondary sulphate contribution was much lower as compared to the level in other urban or rural areas in eastern Canada. Moreover, it was found that the lowest sulphate contribution (3.8%) was in summer and the highest contribution (8.2%) was in spring (Figure 14). Typically, secondary sulphate tends to be abundant in warmer months due to increased photochemical oxidation of SO_2 from local sources or regional transport of fossil-fuel combustion plumes. In Golden, SO_2 concentrations were generally low with average concentrations of 0.63 ppb in winter and 0.21 ppb in summer, reflecting limited availability of the local particulate sulphate precursor in summer. Low sulphate concentration in the summer suggests a negligible influence of local or regional sources and higher mixing heights than during the winter months.

Wood Burning Factor (F3)

The wood burning source was characterized by OC2, OC3, OP, EC1, nitrate, and K in the factor profiles. This factor exhibited the highest source contribution at approximately 34% (3.9 ± 4.1 μg m^{-3}) of the $PM_{2.5}$ mass on average. Water soluble potassium is often considered to be a tracer of biomass combustion. The source profile was composed of large amounts of the total carbonaceous material: OC2(22%), OC3 (37%), OC4(31%), OP(37%), EC1(47%); however, OC1 and EC2 contributed insignificant amounts to this factor. As shown in Table 3, the factor was highly correlated with all biomass burning-related components: high levoglucosan concentrations, black carbon (AE-BC), and UV-absorbing carbon (AE-UV). The presence of levoglucosan indicated the factor was strongly associated with primary particles from wood smoke (Simoneit 1999; Schauer 2001). Overall Spearman correlations of gaseous pollutants with the wood burning source were also high, especially for NO. This indicates that the wood burning source in Golden strongly influenced the increase of not only particulate matter, but also of gaseous pollutants. The contributions of the wood burning source in the winter and in the summer accounted for around 40% and 18% of the total $PM_{2.5}$ mass, respectively, with a winter to summer ratio of 6.4 in mass concentrations.

Wood Processing Factor (F4)

The fourth factor in Figure 13 was characterized by a majority of the Pb (63%), Mn (54%), Cr (61%), Sr (52%), and some sulphate (22%). This factor was attributed to wood processing and accounted for 12.8 % (1.5 ± 1.1 μg m^{-3}) of the total $PM_{2.5}$ on average. The largest industrial source in Golden was a veneer and plywood mill facility, Louisiana Pacific (LP), located in the north region of the Golden monitoring site. According to the 2005 National Pollutant Release Index (NPRI), the dominant emission pollutants from the facility were methanol, lead, and sulphuric acid. Plywood making processes involving drying and pressing with solvents and glues are associated with high VOC emissions. Table 4 shows the correlation analysis between the wood processing source and VOCs. The highest correlations (Spearman *r*) with this factor were found with acetone (0.66), 2-butanol (0.60), ethanol (0.51), and methanol (0.33).

Table 3. Spearman rank coefficients (*r*) for the correlation of resolve source contributions with ambient pollutants, ambient temperature, levoglucosan and the number of vehicles observed in Golden.

	F1	F2	F3	F4	F5	F6	F7
PM_{10}	0.18	0.20	0.25	0.39	**0.75**	0.04	0.17
$PM_{2.5}$	0.05	0.38	**0.60**	0.02	0.41	0.13	0.55
O_3	0.02	0.04	-0.52	0.30	0.18	-0.21	-0.38
CO	0.13	0.24	0.48	-0.28	-0.04	-0.02	0.58
NO	0.04	0.21	**0.64**	-0.30	0.15	0.18	0.55
NO_2	0.15	0.32	0.51	-0.18	0.32	0.06	**0.65**
SO_2	0.08	0.31	0.45	-0.05	0.26	-0.03	0.42
AE-BC	-0.03	0.31	**0.72**	-0.24	0.28	0.05	0.56
AE-UV	-0.03	0.36	**0.77**	-0.31	0.26	0.00	**0.60**
Temperature	-0.12	-0.41	-0.53	0.55	-0.07	0.07	-0.63
Levoglucosan	0.45	0.07	**0.85**	-0.15	0.00	-0.41	**0.75**
Vehicle Density	-0.06	-0.32	-0.67	0.16	0.08	0.24	-0.63

Correlation coefficients higher than 0.6 are shown in bold.

Crustal Material Factor (F5)

The crustal factor, with high loadings of Al, Ca, Fe, Mg, and Si, contributed 9.2% (1.1 ± 1.4 μg m^{-3}) to the $PM_{2.5}$ mass. The source was attributed to a combination of soil and road dust. As expected, the factor was highly correlated with the PM_{10} mass since most of the mass of crustal elements is found in coarse particles. The time series plot of this factor showed large peaks during the spring months especially in March with a contribution of approximately 15% of the $PM_{2.5}$ mass, as compared to the lowest contribution (6%) in fall and winter months. In order to find the most probable direction for the location of the identified sources, Conditional Probability Function (CPF) plots were created for the seven sources (Figure 16). As discussed previously, since wind direction in Golden was highly impacted by topography: more than 80% of wind was from the northwest and the southeast, the CPF plots only provided limited insight into the likely source locations. As shown in the polar plot for the CPF analysis of the crustal factor, high source contribution was more likely related to an easterly wind direction. The Golden monitoring site was located close to the westside of Highway 95 and the Trans Canada Highway junction along with railroads. It appears that the crustal factor was mostly due to road

dust that was redistributed by mobile traffic sources.

Traffic Factor (F6)

The traffic factor was characterized by high loadings of EC2 (84%), EC3(96%), Zn (21%) and Fe (20%). These components were associated with motor vehicle emissions and potentially with locomotives. The Trans Canada Highway, Highway 95, and train railroads were to the east-northwest and southeast-northwest of the Golden site and a large railway yard was located to the south. Particles containing Zn and Fe can be attributed to wear of brake linings and tires as well as from lubricating oils of motor vehicles (Fergussion and Kim 1991; Ristovski et al. 1999; Sternbeck et al. 2002). The traffic factor accounted for 11.8 % (1.4 ± 1.1 μg m^{-3}) of the total $PM_{2.5}$ on average. The source contribution rose in July and August, consistent with the temporal trend of vehicle number as shown in Figure 8. While the correlation coefficient of the motor vehicle factor with the number of vehicles counted in 2005 was around 0.26, the correlation was statistically improved when the factor was compared against the vehicle counts in summer months (June to August 2005, 22 samples) with a coefficient of 0.46. Interestingly, overall correlations between this factor and typical traffic-related gases, (i.e., NO) were poor, possibly due to the strong seasonal variability of the gaseous pollutants associated with the wood burning source. However, the correlation between this factor and typical diesel exhausts: BC and NO, was significantly stronger in summer ($r = 0.54$ for BC, $r = 0.49$ for NO) than the correlation in winter ($r = -0.28$ for BC and $r = 0.04$ for NO). The CPF plot for the traffic factor points to the southwest/southeast suggesting an impact from the Highways and the locomotive switch yard located about 1 km south of the monitoring site.

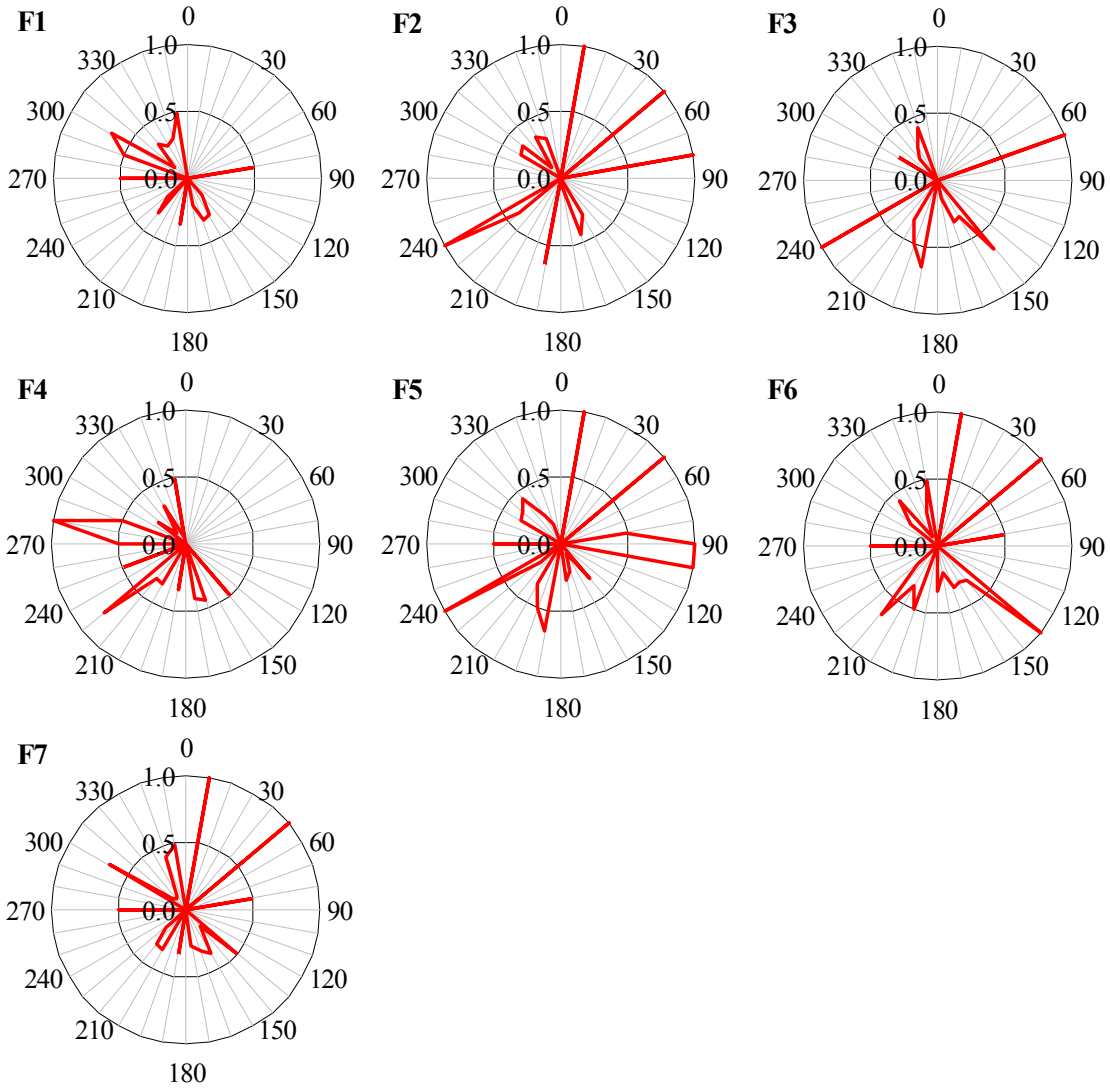

Figure 16. Polar plots of the conditional probability function (CPF) for the highest 20% of the mass contributions from the 7 resolved sources; F1: road salt, F2: sulphate, F3: wood burning, F4: wood processing, F5: crustal, F6: traffic, F7: winter heating.

Table 4. Correlation Analysis between the PMF resolved seven factors and VOCs in Golden.

	F1	F2	F3	F4	F5	F6	F7		F1	F2	F3	F4	F5	F6	F7		F1	F2	F3	F4	F5	F6	F7
1,1,1-Trichloroethane	-0.18	-0.04	-0.19	0.33	0.26	-0.27	-0.44	3-Methyl-1-pentene	0.10	0.08	0.00	0.09	-0.12	0.31	0.49	Ethane	0.28	0.44	0.31	-0.35	-0.02	0.32	**0.60**
1,2,3-Trimethylbenzene	0.15	0.14	0.12	0.24	0.03	0.40	0.40	3-Methylheptane	0.06	0.14	0.18	0.09	0.00	0.42	0.39	Ethanol	0.06	-0.38	-0.29	**0.51**	0.08	0.12	-0.10
1,2,4-Trimethylbenzene	0.14	0.09	0.20	0.16	0.07	0.42	0.33	4-Ethyltoluene	0.12	0.15	0.23	0.18	0.09	0.45	0.35	Ethylacetate	0.15	-0.27	0.09	0.40	0.08	0.25	-0.11
1,2-Dichloroethane	0.36	0.27	-0.30	0.25	0.12	0.01	0.42	4-Methylheptane	0.07	0.16	0.11	0.14	0.02	0.39	**0.50**	Ethylbenzene	0.06	0.13	0.34	0.00	0.06	**0.50**	0.42
1,2-Dichloropropane	0.38	0.25	-0.22	-0.02	-0.01	0.09	**0.58**	Acetaldehyde	0.18	-0.02	0.03	0.36	0.01	0.14	0.13	Ethylene	0.20	0.33	0.44	-0.45	-0.01	0.44	**0.63**
1,2-Diethylbenzene	0.28	0.14	-0.09	0.26	-0.07	0.41	0.48	Acetone	0.04	-0.14	-0.15	**0.66**	0.16	0.13	-0.01	Hexanal	0.29	-0.26	-0.30	0.38	0.07	-0.34	-0.47
1,3,5-Trimethylbenzene	0.16	0.09	0.22	0.13	0.05	0.41	0.32	Acetonitrile	0.02	-0.51	-0.12	0.37	0.08	0.10	0.01	Hexane	0.07	0.29	0.17	0.20	0.13	0.42	0.45
1,3-Butadiene	0.23	0.33	0.40	-0.38	-0.02	0.46	**0.63**	Acetylene	0.22	0.32	0.42	-0.42	-0.03	**0.51**	**0.67**	Isobutane	0.06	0.44	0.27	0.00	0.16	0.32	0.49
1,3-Diethylbenzene	0.20	0.18	0.24	0.13	0.00	0.42	0.38	Acrolein (2-Propenal)	0.25	0.29	0.42	-0.13	-0.20	0.21	0.37	iso-Butylbenzene	0.07	0.09	0.04	0.31	0.00	0.29	0.36
1,4-Dichlorobenzene	0.17	-0.01	0.01	0.40	-0.04	0.26	0.05	a-Pinene	-0.07	0.07	0.18	0.46	0.38	0.27	-0.02	Isoprene	-0.32	-0.17	-0.08	0.39	0.20	0.11	-0.28
1,4-Diethylbenzene	0.39	0.00	-0.23	0.34	-0.12	0.26	0.41	Benzaldehyde	0.31	-0.42	-0.15	0.34	-0.13	-0.11	-0.29	Isopropyl Alcohol	0.12	-0.55	-0.14	0.31	-0.12	0.39	0.13
Butyl alcohol	0.33	-0.44	-0.16	0.37	0.02	0.02	-0.20	Benzene	0.25	0.30	0.46	-0.36	0.00	**0.54**	**0.67**	iso-Propylbenzene	0.18	0.27	0.29	-0.05	-0.06	0.48	**0.59**
1-Butene/Isobutene	0.21	0.29	0.27	-0.10	-0.02	0.46	**0.60**	b-Pinene	-0.15	-0.16	0.13	0.37	0.21	0.06	-0.39	m and p-Xylene	0.06	0.11	0.24	0.13	0.09	0.45	0.37
1-Butyne	0.15	0.29	0.38	-0.42	-0.06	0.45	**0.65**	Bromoform	0.26	0.22	0.28	-0.42	0.05	0.37	**0.62**	2-Methyl-2-propenal	0.08	-0.33	-0.11	**0.56**	0.24	0.32	0.03
1-Methylcyclohexene	0.07	0.21	0.24	-0.09	-0.03	0.48	0.46	Bromomethane	-0.12	-0.04	-0.40	**0.57**	0.37	-0.26	-0.30	MEK	0.28	0.02	0.26	0.42	-0.15	0.30	0.06
1-Methylcyclopentene	0.00	0.10	0.25	0.04	0.07	0.43	0.38	Butane	0.13	0.30	0.30	0.05	0.26	0.48	0.49	Methanol	-0.16	-0.28	-0.03	0.33	-0.01	0.33	0.08
1-Octene	-0.07	0.01	-0.34	0.43	0.16	-0.15	0.10	Butylaldehyde	0.31	-0.19	-0.20	0.36	-0.15	-0.06	-0.02	Methyl Acetate	0.07	0.29	**0.63**	-0.18	0.05	0.29	0.24
1-Propyne	0.12	0.37	**0.50**	-0.49	-0.01	0.37	**0.50**	Camphene	-0.11	0.11	0.10	**0.51**	0.25	-0.04	-0.26	MIBK	0.30	-0.30	0.02	0.47	-0.08	0.21	-0.03
2,2,3-Trimethylbutane	-0.04	0.10	-0.25	0.49	0.18	0.13	0.14	Carbon Disulfide	0.19	-0.43	-0.33	0.44	-0.17	0.03	-0.02	MVK	0.10	-0.38	-0.03	**0.57**	0.11	0.25	-0.09
2,2,4-Trimethylpentane	0.03	0.02	0.12	0.19	0.04	0.46	0.32	Carbontetrachloride	0.02	-0.10	-0.22	0.32	0.26	-0.06	-0.22	Naphthalene	0.13	0.31	0.30	-0.10	0.01	0.48	0.41
2,2,5-Trimethylhexane	0.11	0.13	0.22	0.09	0.00	0.46	0.37	Chlorobenzene	0.28	0.05	-0.30	0.19	0.01	0.39	**0.52**	n-Butylbenzene	0.09	0.17	0.22	0.16	0.00	0.42	0.44
2,2-Dimethylpentane	0.03	0.20	0.02	0.30	0.16	0.27	0.29	Chloroethane	0.12	-0.04	-0.22	0.38	-0.19	-0.04	-0.02	n-Propylbenzene	0.14	0.14	0.21	0.17	0.00	0.46	0.38
2,2-Dimethylpropane	0.47	0.30	-0.05	0.12	0.12	0.34	**0.62**	Chloroform	0.00	0.08	0.03	0.47	0.35	0.16	-0.08	Octane	0.07	0.19	0.16	0.15	-0.01	0.39	0.41
2,3,4-Trimethylpentane	0.05	0.07	0.16	0.12	-0.02	0.46	0.34	Chloromethane	-0.06	-0.03	-0.53	0.46	0.27	-0.27	-0.11	o-Xylene	0.08	0.11	0.24	0.10	0.07	0.48	0.40
2,3-Dimethylpentane	0.05	0.11	0.17	0.15	0.07	0.41	0.28	cis-1,2-Dimethylcyclohexane	0.27	0.17	0.01	0.14	-0.04	**0.54**	**0.71**	p-Cymene	0.10	0.16	0.14	0.45	0.26	0.34	0.35
2,4-Dimethylhexane	0.06	0.11	0.14	0.13	0.02	0.46	0.39	cis-1,3-Dimethylcyclohexane	0.10	0.22	0.21	0.14	0.04	0.45	0.38	Pentane	0.03	0.15	0.15	0.22	0.12	0.44	0.40
2,5-Dimethylhexane	0.09	0.11	0.18	0.12	0.00	0.44	0.36	cis-2-Butene	0.11	0.13	0.31	0.00	0.12	**0.56**	**0.55**	Propane	0.12	0.25	0.25	-0.12	0.14	**0.54**	**0.67**
2-Butanol	0.35	-0.47	-0.32	**0.60**	-0.03	0.00	-0.31	cis-2-Pentene	-0.01	-0.02	0.17	0.18	0.15	0.44	0.27	Propyl alcohol	0.28	-0.20	-0.31	0.41	0.04	-0.26	-0.21
2-Ethyltoluene	0.14	0.15	0.25	0.13	0.02	0.47	0.37	cis-3-Methyl-2-pentene	-0.02	0.03	0.16	0.12	0.12	0.47	0.37	Propylene	0.22	0.30	0.38	-0.36	-0.03	0.46	**0.63**
2-Methyl-1-butene	0.08	0.05	0.14	0.16	0.15	0.46	0.38	cis-4-Methyl-2-pentene	-0.05	0.00	0.20	0.18	0.13	0.45	0.27	sec-Butylbenzene	0.12	0.14	0.08	0.26	0.04	0.37	0.43
2-Methyl-2-butene	-0.01	-0.01	0.20	0.17	0.13	0.45	0.24	Cyclohexanone	0.26	-0.21	-0.26	**0.52**	-0.15	-0.13	-0.19	Styrene	0.20	0.23	0.32	-0.12	0.04	0.48	0.48
2-Methylbutanal	0.43	-0.26	-0.08	**0.57**	0.02	0.01	-0.37	Cyclohexene	0.10	0.06	-0.26	0.20	-0.13	0.07	0.39	Tetrachloroethylene	0.20	0.26	0.11	0.04	0.12	0.40	**0.57**
2-Methylfuran	0.25	0.32	**0.54**	-0.43	-0.32	0.08	0.27	Cyclopentene	0.04	0.09	0.29	0.06	0.06	0.48	0.40	Toluene	0.09	0.22	0.40	-0.02	0.07	0.48	0.39
2-Methylheptane	0.10	0.12	0.10	0.13	-0.05	0.40	0.40	Decane	0.03	0.28	0.15	0.41	0.06	0.18	0.12	trans-1,4-Dimethylcyclohexane	0.10	0.20	0.20	0.11	0.03	0.46	0.40
2-Methylpentane	-0.05	0.07	0.03	0.30	0.10	0.34	0.32	Dibromochloromethane	0.14	0.08	-0.14	0.04	0.14	0.14	0.47	trans-2-Butene	0.22	0.17	0.36	-0.10	0.11	**0.64**	**0.66**
2-Pentanone	0.14	-0.13	0.31	0.25	-0.02	0.40	0.19	Dichloromethane	0.04	0.05	-0.16	0.46	0.21	-0.01	0.14	trans-2-Hexene	-0.02	0.00	0.20	0.13	0.12	0.42	0.27
3-Ethyltoluene	0.14	0.13	0.23	0.16	0.05	0.46	0.37	d-Limonene	0.23	0.03	-0.27	0.30	-0.14	0.18	0.36	trans-2-Octene	0.03	0.29	0.21	0.11	0.06	0.49	0.47
3-Methyl-1-butene	0.06	0.15	0.33	0.06	0.12	0.49	0.40	Dodecane	-0.22	0.05	-0.26	**0.53**	0.24	-0.17	-0.37	trans-2-Pentene	-0.02	-0.02	0.18	0.21	0.18	0.46	0.25

Winter Heating Factor (F7)

The winter heating factor was characterized by high concentrations of OC1 mass (91%) as well as acetate and nitrate. The factor was identified as the second largest source, accounting for 26% (3.0 ± 4.6 μg m^{-3}) of the $PM_{2.5}$ on average. The time series plot for the winter heating source clearly displayed a significant difference in the contributions between heating months (November to March) and non-heating months (May to August). The heating months/non-heating months ratios for the contributions of the winter heating factor (F7) and the wood burning factor (F1) were about 8.7 and 5.3, respectively. The higher ratio suggests that the winter heating source was more strongly dependent on season. The loading of water soluble potassium, a biomass burning marker, was lower compared to that in the wood burning factor. In addition, the correlation between the winter heating factor and levoglucosan was also lower than the correlation for the wood burning factor. However, NO_2 exhibited the highest correlation with this factor, and it was inversely associated with ambient temperature as shown in Table 3. It was speculated that the winter heating factor was associated with secondary productions from the reaction of primary emissions from winter heating activities, i.e., wood burning and gas furnace burning, and was more likely related to temperature inversion events during the heating season. Data was not available to identify the occurrence of temperature inversions in 2005. Instead, very low wind speed was used as an indirect indicator of inversion events. Table 5 shows the ratio of resolved source contributions at low wind speeds (<1.0 m/sec) to the contributions at high wind speed (>1.5 m/sec). Twenty-nine of total available samples (173 days) were classified as the very low wind speed days, and more than 90% of the low wind days were observed during November to February. The contribution ratio for this factor was higher than the ratio for the wood burning source as shown in Table 5. This supports the idea that this factor was accentuated by secondary organics in the stagnant air masses in the winter. Alkene and alkane, including acetylene, benzene, propane, 1,3-butadiene, propylene, ethane and ethylene, were highly correlated with the winter heating source; the Spearman r values were all higher than 0.6. The high correlation with less-reactive alkanes, propane (r =0.67) and ethane (r =0.60) may indicate that primary aerosol from local biomass burning sources were oxidized and significantly accumulated during the temperature inversion days in the winter. The contribution of the winter heating factor potentially reflects the variability of secondary organics and/or aged

particles from winter heating sources in stagnant conditions.

Table 5. Comparison of the seven source contributions (μg m^{-3}) at the low and high wind speeds.

Wind Speed	F1	F2	F3	F4	F5	F6	F7
< 1.0 m/sec	0.12	0.25	**0.60**	0.11	0.35	0.22	**0.73**
> 1.5 m/sec	0.14	0.20	**0.26**	0.12	0.21	0.20	**0.20**
Ratio	0.87	1.30	**2.28**	0.95	1.69	1.07	**3.67**

F1: road salt, F2: sulphate, F3 : wood burning, F4: wood processing, F5: crustal material, F6 : traffic, F7: winter heating

3.6.3 Comparison of PMF and EPA PMF Results

As expected, EPA PMF created the seven factor solution consistent with the PMF analysis. In order to find the global minimum of the Q value, the EPA PMF model was run 100 times with the error constant (*C3*) of 10%. Similar to the PMF results, stable Q values were observed at values of 4262, 4299, and 4307. The source profile and contributions for the three Q values were reasonably close, suggesting the uncertainties from the EPA PMF analysis were properly estimated. In this study, most of the scaled residuals were between -3 to +3 and only 14 of the total 174 samples were somewhat beyond the range. To estimate the uncertainty of the EPA PMF seven factor solution, 500 bootstrap runs with a correlation of 0.70 were performed. For most factors the bootstraps were mapped to the respective base case factor, with the exception of the traffic factor for which 18% of the runs were not mapped to the original factor. The EPA PMF analysis also provided graphical results illustrating the uncertainties in the species for each profile by percent of species and concentration. Box whisker plots for the seven identified factors with their uncertainties are presented in the Appendix section.

The source contributions resolved by EPA PMF and PMF are shown in Figure 17. As described previously, the source contributions were estimated by using the multilinear regression coefficients. Agreement between the two models was quite good with respect to the source

contributions and the profiles of the sources as shown in Figure 18. Average source contributions as an average $PM_{2.5}$ mass were close for the two models for all factors. The EPA PMF analysis shows that the most important $PM_{2.5}$ sources in Golden were wood burning (33%), winter heating (28%), wood processing (11%), traffic (11%), crustal material (10%), secondary sulphate (6%), and road salt (1%) on average. In the EPA PMF analysis, the linear correlation coefficient (r^2) between predicted and measured concentration for each species over all samples was approximately 0.939 with a slope of 0.931, suggesting that the resolved factors from the EPA PMF analysis effectively reproduced the original mass concentration.

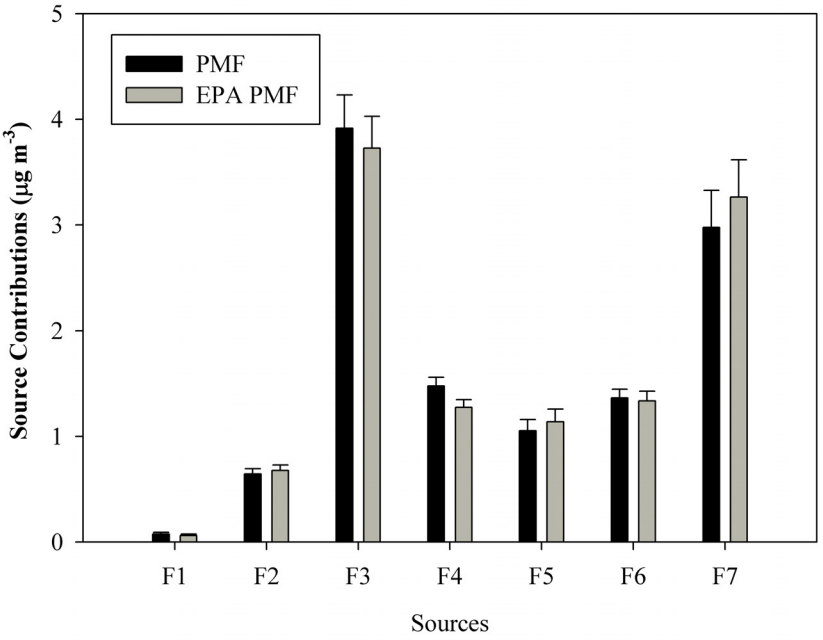

Figure 17. Comparison of average source contributions for the seven factors for PMF and EPA PMF models. F1: road salt, F2: secondary sulphate, F3: wood burning, F4: wood processing, F5: crustal material, F6: traffic, F7: winter heating. The error bars represent the standard errors.

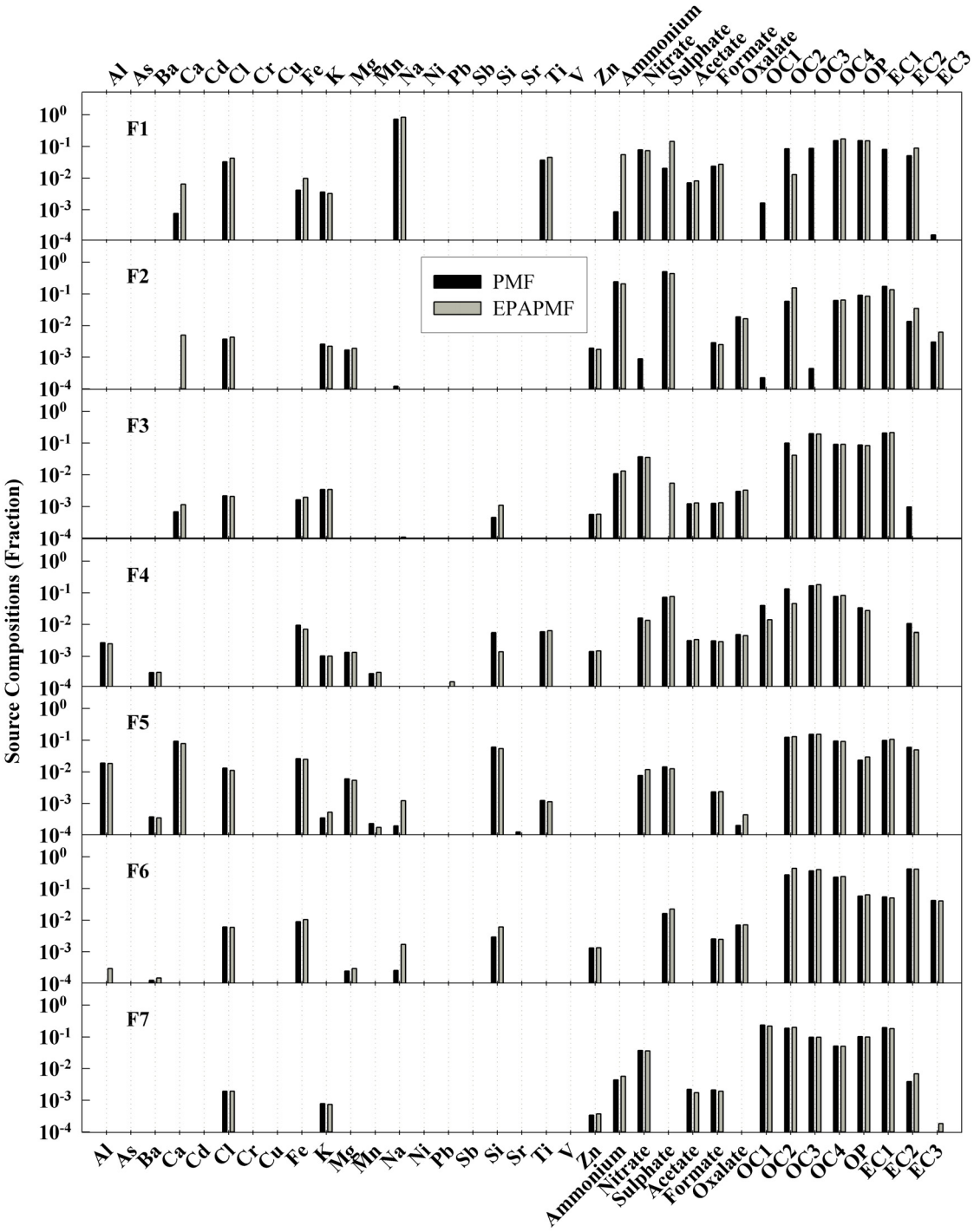

Figure 18. Comparison of source profiles for PMF and EPA PMF models. F1: road salt, F2: secondary sulphate, F3: wood burning, F4: wood processing, F5: crustal material, F6: traffic, F7: winter heating.

4. CONCLUSIONS

The application of the PMF model to the $PM_{2.5}$ speciation data collected from November 2005 to August 2006 in Golden, B.C., Canada resulted in isolating and evaluating the contributions and compositions of seven sources: road salt, secondary sulphate, wood burning, wood processing, crustal material, traffic, and winter heating. The most important isolated factors affecting the deep valley area were found to be consistent with emissions from wood burning and winter heating activities, highly associated with high carbonaceous compound concentrations. The concentrations of water soluble potassium, black carbon and levoglucosan were primarily correlated with the wood burning factor contributions accounting for 3.9 ± 4.1 μg m^{-3} (34%) of the total $PM_{2.5}$ mass on average. The winter heating source, with high OC1 concentration, contributing 3.0 ± 4.6 μg m^{-3} (24%) to the total $PM_{2.5}$ on average, was most affected by the frequent temperature inversions and stagnant air masses that occur in Golden in the winter. The wood burning and winter heating factors were correlated with the concentrations of many VOCs including benzene and 1.3-butadiene. The wood burning and the winter heating factor contributions were significantly higher in the winter than summer months by factors of 6 and 10, respectively. The influence of the wood processing factor, contributing 1.5 ± 1.1 μg m^{-3} (13%) to the total $PM_{2.5}$ mass, tended to increase during summer months by a factor of 2.5 as compared to the winter months. The traffic factor, dominated by EC2 and EC3, contributed 1.4 ± 1.1 μg m^{-3} (12%) and also exhibited increased contribution to the $PM_{2.5}$ levels in the summer than in the winter. This result is consistent with the increase of motor vehicle density on highways in summer months. The crustal material factor accounted for 1.1 ± 1.4 μg m^{-3} (9%) of the $PM_{2.5}$ mass and showed significant seasonality, with a strong spring maximum. The secondary sulphate factor contribution to the $PM_{2.5}$ mass was quite low even during the warm months of the year at this rural site; the contribution was 0.6 ± 0.6 μg m^{-3} (6%) on average. The highest contribution of the sulphate factor was observed in spring with an average of 0.8 ± 0.8 μg m^{-3} (8%). The road salt factor, with sodium and chloride tracer species, was minor in its $PM_{2.5}$ mass contribution, representing approximately 1 % on average.

EPA PMF was also used to analyze the $PM_{2.5}$ speciation data in Golden and the results were

compared with the PMF results. The PMF and EPA PMF models effectively identified common sources and the results agreed well, both in compositions and contributions to $PM_{2.5}$ in Golden during the study period.

5. IMPLICATIONS

This study has demonstrated that speciated filter sampling coupled with receptor modeling, using models such as PMF, can provide quantitative information on the contributions of dominant sources impacting on a site.

As described in the report, application of PMF involves three steps: careful evaluation of the data available, knowledgeable application of the PMF model to resolve factors, and association of each factor with a physically meaningful source, i.e., source identification.

The introduction of the EPA version of PMF has made this type of receptor modeling more accessible to a broader range of users. In this study the EPA version was shown to provide similar results to the more sophisticated model. However, even with the EPA version, deciding on the number of factors that can be supported by the available data still requires experience. In addition, beyond the operation of the model, considerable judgment is still required in the initial data screening and the final source identification.

The capacity to isolate factors is dependent on the quality and quantity of the data available. The relatively comprehensive 22 months of data available for Golden allowed the isolation of seven factors; an additional year of sampling, or more frequent sampling during the 22 months, might have allowed resolution of one or two more factors. Resolution of factors becomes increasingly more difficult as their contributions become smaller.

Initial evaluation and screening of the available data is critical to the quality of the model output. Chemical analysis by multiple methods, as was done for the Golden data, provides benefits in

terms of expanding the number of species included in the data, measurement validation by comparison between the methods, and by allowing selection between methods for difficult to measure species that may only have partially complete sets of results. Although a strength of PMF is that it can account for individual missing or below detection results, a minimum portion of valid results for a given species is still required in order for the species to contribute to the model output.

Association of factor isolated by PMF with sources, source identification, is the step that requires the highest degree of judgment and experience. Correlation of the factors with other available data such as gas concentrations and meteorological data can help along with the calculation of wind direction, diurnal, weekday/weekend and seasonal trends. However, judgment and experience with the sources identified at other locations still play significant roles. The identity of some of the factors found in Golden such as the crustal source was apparent whereas distinction between others such as the wood burning and winter heating was initially less evident.

We recommend that receptor modeling using PMF be applied to sites across Canada in order to fully exploit the benefits of all the NAPS data that has been generated to date. As PMF is applied to a wider range of sites, the steps that require more judgment such as the initial data treatment and final source identification will become more routine, allowing this type of modeling to be undertaken by a broader range of individuals.

6. ACKNOWLEDGMENTS

This work was supported by the Environment Canada under Project Contract K2313-06-0015. The Golden site is part of the NAPS fine particle speciation network currently comprising 13 sites across Canada. This program was initiated in 2003/2004 and its success and the quality of the data generated are a result of substantial method development work undertaken by a number of scientists in the Environmental Science and Technology Centre of Environment Canada in Ottawa. In particular the work of Dr. Ewa Dabek-Zlotorzynska (establishment of the multi-disciplinary laboratory support for the $PM_{2.5}$ chemical speciation network, ion chromatography and ICP-MS), David Mathieu (gravimetric analysis, XRF and all sample handling and preparation activities), Dr. Luyi Ding (organic and elemental carbon) and Dr. Daniel Wang (organic and elemental carbon, VOC and polar VOC) are gratefully acknowledged. B.C. Ministry of Environment (MOE) staff have operated and maintained the instrumentation at the Golden site. Special thanks to Garry Bell and Christopher Marsh for their continued efforts keeping the instrumentation running smoothly. In addition, we gratefully acknowledge the work of Louisiana Pacific, in particular Mike Brygger for the operation of the dichot, speciation and VOC monitor. We thank the City of Golden, the Golden District Golf and Country Club, the Golden Hospital, and Canadian Pacific Railway for their support. Rigorous quality assurance (QA) and quality control (QC) of continuous data was done by the Water, Air Monitoring and Reporting Section of the Environmental Protection Division. We would like to acknowledge the hard work of Sharon Gunter and Ernie Tradewell for data validation and QA. In addition, the project was co-managed by Mark Graham and Paul Willis of MOE. This project would not have been developed if not for the efforts of Paul Willis and others on the Speciation Working Group, who implemented and designed the study. The authors are grateful to Dennis Herod, Mark Graham, Jeff Brook, and Tom Dann for their input throughout the project and providing review comments on this report. Lastly, we wish to acknowledge the assistance of Southern Ontario Centre for Atmospheric Aerosol Research (SOCAAR) colleagues, Andrew Knox, Krystal Godri, Maygan McGuire, Ryan D'Souza, Kelly Sabaliauskas, and Xiaohong Yao.

7. REFERENCES

Andreae, M.O.(1983). Soot Carbon and Excess Fine Potassium: Long-range Transport of Combustion-derived Aerosols. *Science* 220:1148–1151.

Ashbaugh, L.L.,Malm, W.C. and Sadeh, W.Z. (1985). A Residence Time Probability Analysis of Sulfur Concentrations at Grand Canyon National Park. *Atmos. Environ*. 19:1263-1270.

Burnett, R. T., Brook, J., Dann, T., Delocla, C., Philips, O., Cakmak, S., Vincent, R., Goldberg, M. S., and Krewski, D. (2000). Association between Particulate- and Gas-Phase Components of Urban Air Pollution and Daily Mortality in Eight Canadian Cities. *Inhal. Toxicol*. 12(suppl. 4):15-39.

Cadle, S.H. and Mulawa, P.A. (1990). Atmospheric Carbonaceous Species Measurement Methods Comparison Study: General Motors Results. *Aerosol Sci. Tech*. 12:128-141.

Chueinta, W., Hopke, P.K., and Paatero, P. (2000). Investigation of Sources of Atmospheric Aerosol at Urban and Suburban Residential Area in Thailand by Positive Matrix Factorization. *Atmos. Environ.* 34:3319-3329.

Crahan, K., Hegg, D.A., and Covert, D.S. (2004) An Exploration of Aqueous Oxalic Acid Production in 15 the Coastal Marine Atmosphere. *Atmos. Environ*. 38: 3757-3764.

Dockery, D.W., Pope, C.A., Xu, X., Spengler, J.D., Ware, J.H., Fay, M.E., Ferris, B.G., and Speizer, F.E. (1993). An Association between Air Pollution and Mortality in Six US Cities. *New Engl. J. Med.* 329:1753-1759.

Eberly S. (2005). EPA PMF 1.1 User's Guide. Prepared by the U.S. Environmental Protection Agency, National Exposure Research Laboratory, Research Triangle Park, NC, June.

Efron, B. and Tibshirani, R.J.(1993). An Introduction to the Bootstrap; Monographs on Statistics and Applied Probability, No.57; Chapman and Hall: New York.

Environment Canada (2005a). Climate Data Online, Canada. (http://www.climate.weatheroffice.ec.gc.ca/climateData/canada_e.html)

Environment Canada (2005b). National Pollutant Release Inventory (NPRI) 2005, Canada. (http://www.ec.gc.ca/pdb/querysite/query_e.cfm)

Fergussion, J.E. and Kim, N.D. (1991). Trace Elements in Street and House Dust: Source and Speciation. *Sci. Total Environ.* 100:125-150.

Jenkins, B.M., Jones, A.D., Turn, S.Q. and Williams, R.B. (1996). Particle concentrations, gas-particle partitioning, and species intercorrelations for polycyclic aromatic hydrocarbons (PAH) emitted during biomass burning. *Atmos. Environ*. 30: 3825-3835.

Jeong, C.-H., Hopke, P.K., Kim, E., and Lee, D.W. (2004). The comparison between thermal-optical transmittance elemental carbon and Aethalometer black carbon measured at multiple monitoring sites. *Atmos. Environ.* 38: 5193-5204.

Lee, K. H. P, Brook, J. R., Dabek-Zlotorzynska, E., and Mabury. S. A. (2003). Identification of the Major Sources Contributing to $PM_{2.5}$ Observed in Toronto. *Environ. Sci. Technol.* 37:4831-4840.

Ma, Y., Weber, R.J., Lee, Y.-N, Orsini, D.A., Maxwell-Meier, K., Thornton, D.C., Bandy, A.R., Clarke, A.D., Blake, D.R., Sachse, G.W., Fuelberg, H.E., Kiley, C.M., Woo, J.-H., Streets, D.G., and Carichael, G. R. (2003). Carmichael Characteristics and Influence of Biosmoke on the Fine-particle Ionic Composition Measured in Asian Outflow During the Transport and Chemical Evolution Over the Pacific (TRACE-P) Experiment. *J. Geophys. Res.*, 108(D21), 8816, doi:10.1029/ 2002JD003128.

Paatero, P. (1997). Least Square Formulation of Robust, Non-Negative Factor Analyzer. *Chemom. Intell. Lab. Syst.* 37:23-35.

Paatero, P. (1998). User's Guide for Positive Matrix Factorization Programs PMF2 and PMF 3.

Paatero, P. (1999). The Multilenear Engine - A Table-Driven Least Squares Program for Solving Multilinear Problem, Including the n-way Parallel Factor Analysis Model. *J. Computational. Graphical. Stat*. 8:854-888.

Paatero, P., Hopke, P.K., Song, X.H., Ramadan, Z. (2002). Understanding and Controlling Rotations in Factor Analytic Models. *Chemom. Intell. Lab. Syst*. 60: 253-264.

Paatero, P. and Hopke, P.K. (2003). Discarding or Downweighting high-Noise Variables in Factor Analytic Models. *Analytica Chimica Acta* 490: 277-289.

Polissar, A.V., Hopke, P.K., Malm, W.C., and Sisler, J.F. (1998). Atmospheric Aerosol over Alaska: 2. Elemental Composition and Sources. *J. Geophys. Res*. 103:19045-19057.

Polissar, A.V., Hopke, P.K., and Poirot, R.L. (2001). Atmospheric Aerosol over Vermont: Chemical Composition and Sources. *Environ. Sci. Technol.* 35:4604-4621.

Ristovski, Z., Agranovski, V., Bostrom, T., Thomas, S., Hitchins, J., and Morawska, L. (1999).

Elemental Composition of Combustion Emissions from Spark Ignition Vehicles. *J. Aerosol Sci*. 30 (Suppl.1):S845-S846.

Schauer, J.J., Kleeman, M.J., Cass, G.R., and Simoneit, B.R.T. (2001). Measurement of Emissions from Air Pollution Sources. 3. C1-C29 Organic Compounds from Fireplace Combustion of Wood. *Environ. Sci. Technol.* 35: 1716-1728.

Simoneit, B.R.T., Schauer, J.J., Nolte, C.G., Oros, D.R., Elias, V.O., Fraser, M.P., Rogge, W.F., and Cass, G.R. (1999). Levoglucosan, A Tracer for Cellulose in Biomass Burning and Atmospheric Particles. *Atmos. Environ*. 33:173-182.

Sternbeck, J., Sjödin, Å., and Andréasson, K. (2002). Metal Emissions from Road Traffic and the Influence of Resuspension: Results from Two Tunnel Studies. *Atmos. Environ.* 36:4735-4744.

8. APPENDIX : EPA PMF Bootstrapping Results

Uncertainties of species for the seven factor profiles resolved by running bootstraps of the EPA PMF analysis are detailed in this section. The selected final Q value(robust) was 4262. In order to find a high confidence level, the bootstrapping method was run 500 times with a correlation of 0.70. Asterisks in the box whisker plots for each profile denote with the original run. Red symbols represent outliers beyond the 25th to 75th percentile range. The black boxes indicate where the 50th percentile of the bootstrap runs lie.

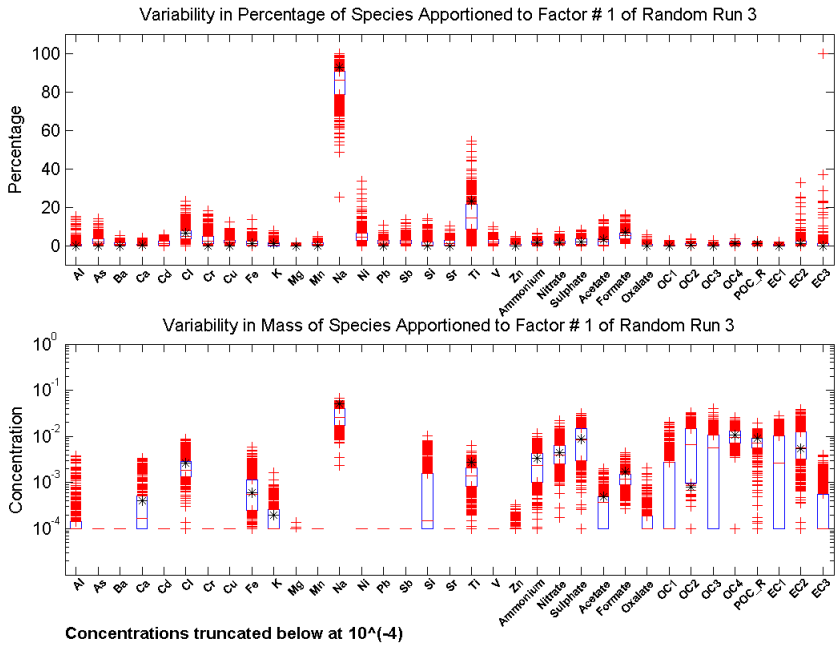

Uncertainty for the components of the road salt factor (F1).

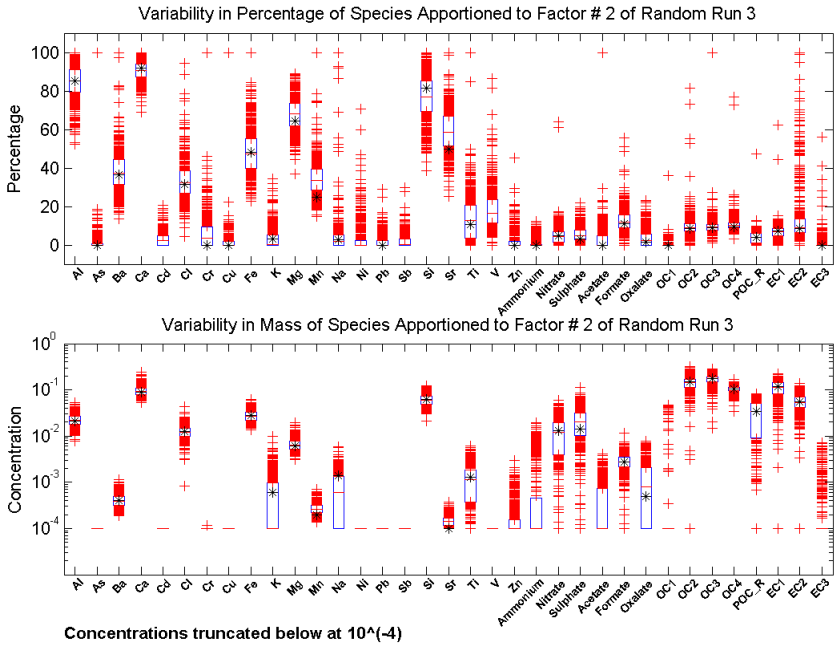

Uncertainties for the components of the crustal material factor (F2).

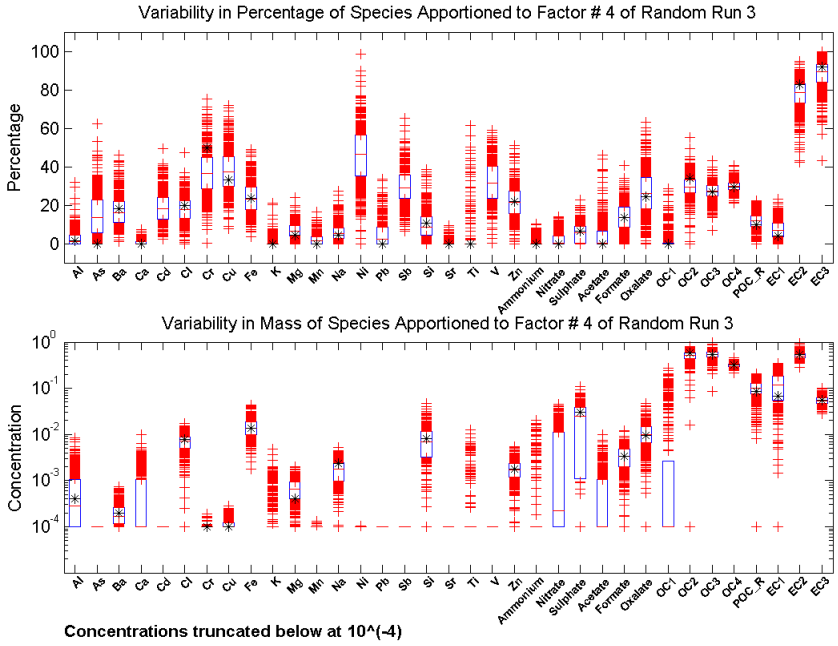

Uncertainties for the components of the traffic factor (F3).

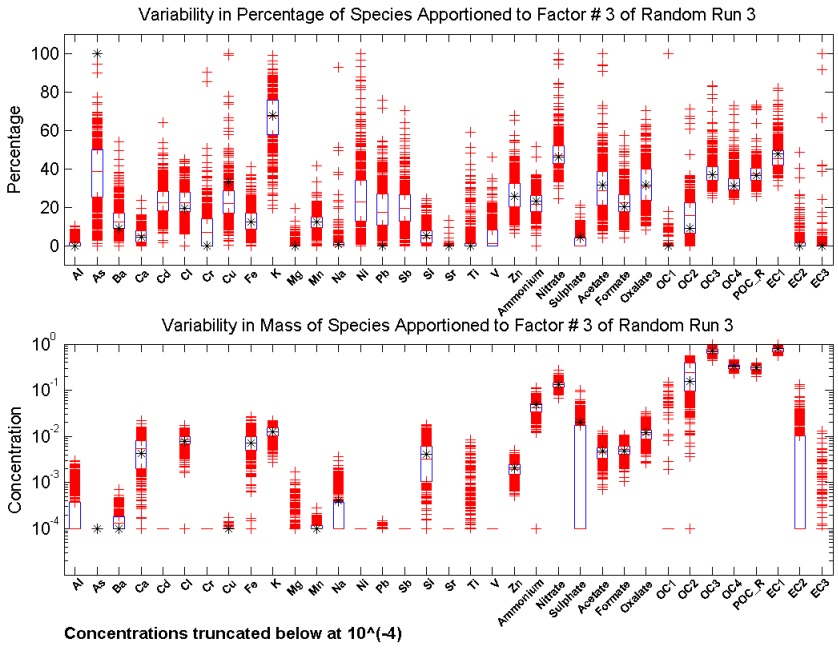

Uncertainties for the components of the wood burning factor (F4).

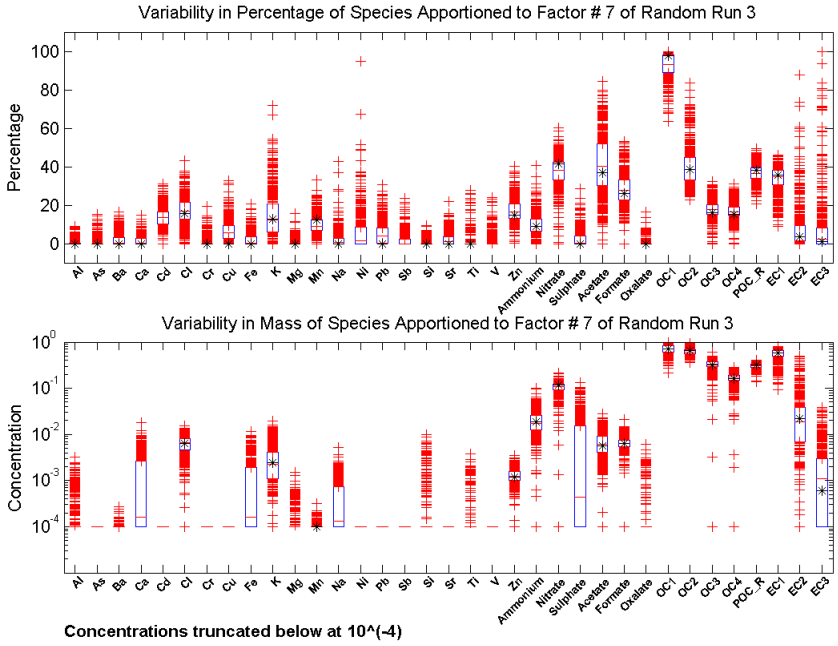

Uncertainties for the components of the winter heating factor (F5).

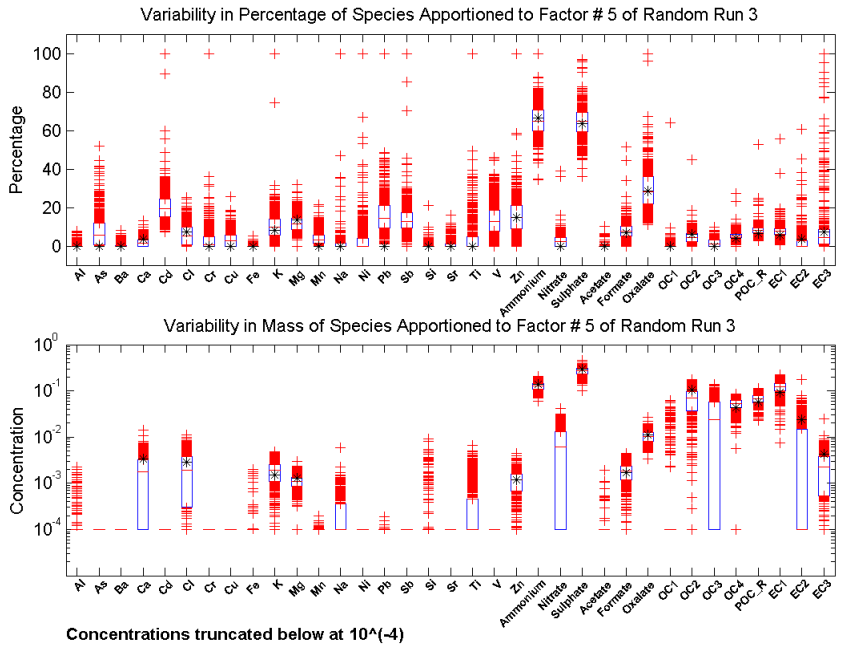

Uncertainties for the components of the secondary sulphate factor (F6).

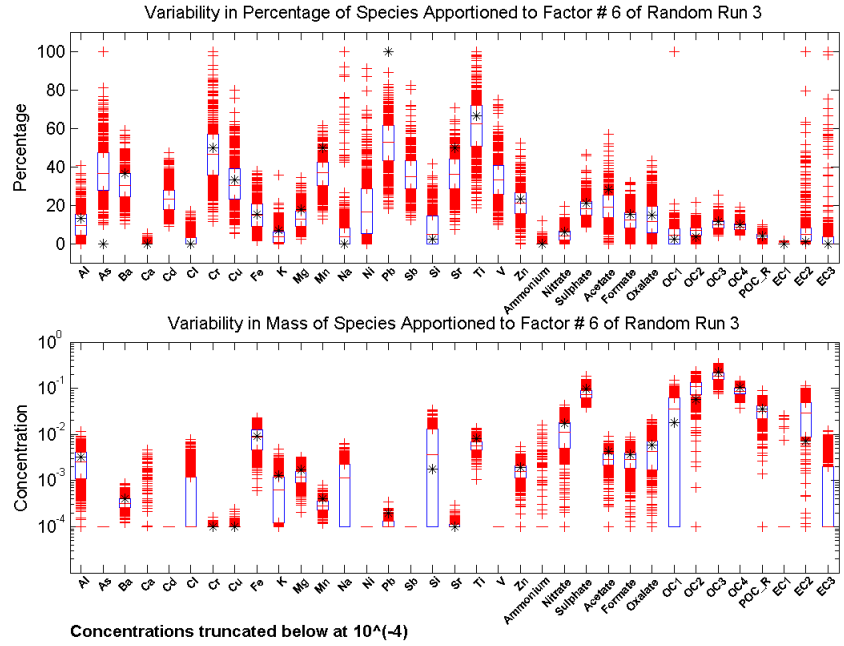

Uncertainties for the components of the wood processing factor (F7).